Biomedicine & Pharmacotherapy 200 (2026) 119530

Contents lists available at ScienceDirect

Biomedicine & Pharmacotherapy

journal homepage: www.elsevier.com/locate/biopha

A small molecule voltage-sensor modulator enhances the function of the cardiac $Na_V1.5$ channel

Geraldo Jorge Domingos [a], Adam Feher [a,b,c], Russo Teklu Teshome [a], Shahrukh Husain [a], Ferenc Papp [a], Al Olaimi Amna [a], Kavya C. Bangera [a], Zsigmond Vizi [a], Rama Elian [a], Zsigmond Máté Kovács [d], Norbert Szentandrássy [d,e], Martina Piga [f], Tihomir Tomašič [f], Nace Zidar [f], Zoltan Varga [a,*]

[a] Department of Biophysics and Cell Biology, Faculty of Medicine, University of Debrecen, Egyetem tér 1, Debrecen 4032, Hungary
[b] Department of Biochemistry and Molecular Biology, The University of Chicago, 929 E 57th St, Chicago, IL 60637, USA
[c] Center for Mechanical Excitability, The University of Chicago, A929 E 57th St, Chicago, IL 60637, USA
[d] Department of Physiology, Faculty of Medicine, University of Debrecen, Egyetem tér 1, Debrecen 4032, Hungary
[e] Department of Basic Medical Sciences, Faculty of Dentistry, University of Debrecen, Egyetem tér 1, Debrecen 4032, Hungary
[f] Department of Pharmaceutical Chemistry, Faculty of Pharmacy, University of Ljubljana, Aškerčeva cesta 7, Ljubljana 1000, Slovenia

ARTICLE INFO

Keywords:
Voltage-gated ion channels
Voltage-sensor domain
Activation kinetics
Gating modulator
NaV1.5 channel activation
Brugada mutation
Enhanced charge transfer

ABSTRACT

The development of new drug molecules targeting voltage-gated ion channels has declined in the last decade, highlighting the need for novel lead compounds with new mechanisms of action. We previously identified NZ-58 as a small-molecule inhibitor of the H_V1 proton channel. At 50 μM NZ-58 also potently blocked voltage-gated Na^+ and K^+ channels, but not the non-voltage-gated ones, suggesting an interaction with the voltage-sensor domains (VSDs). At lower concentrations (0.5–10 μM), it altered gating kinetics with minimal amplitude changes. NZ-58 significantly slowed the current activation kinetics of the channels, as well as the VSD-linked fast inactivation of the $Na_V1.5$ channel, thereby substantially increasing total charge transfer. The loss-of-function Brugada mutant $Na_V1.5$-R1632C was similarly enhanced by NZ-58, but the effect was not present on slowly inactivating K_V channels. Gating current measurements confirmed a direct effect on VSD movement. The voltage-dependence of activation and steady-state inactivation were not altered in $Na_V1.5$, but its recovery from inactivation was slowed. NZ-58 was able to bind to the channels in the closed state, not requiring the activated conformation of the VSDs, and it could exert its effects when applied from either side of the membrane. Being non-selective, NZ-58 is not an ideal lead compound for therapeutic ion channel modulation. However, considering that many clinically used ion channel modulators are multi-target "dirty drugs" that still achieve therapeutic benefit, and the unique features of its interactions with voltage-gated channels, we suggest that NZ-58 is worthy of further investigations as a prospective ion channel modulator lead compound.

1. Introduction

Voltage-gated ion channels (VGICs) establish permeation pathways for ions across the plasma membrane controlled by the cellular membrane potential. Voltage-gated cation channels permeable for Na^+ (Na_V), K^+ (K_V) and Ca^{2+} (Ca_V) are essential for generating action potentials in excitable cells, but they are also extensively expressed by non-excitable cells where they control a plethora of cellular functions such as volume-, pH- or osmoregulation, transport mechanisms and many others via regulating the membrane potential [1,2]. VGICs share a highly homologous overall structure comprising four identical or very similar subunits in homo- and hetero-tetrameric K_V channels and a

* Corresponding author.
E-mail addresses: domingosgeraldo@med.unideb.hu (G.J. Domingos), adamfeher@uchicago.edu (A. Feher), russo.teklu@med.unideb.hu (R.T. Teshome), husain.shahrukh@med.unideb.hu (S. Husain), papp.ferenc@med.unideb.hu (F. Papp), amna.alolaimi@med.unideb.hu (A.O. Amna), kavya@mailbox.unideb.hu (K.C. Bangera), zsigavizi@mailbox.unideb.hu (Z. Vizi), gaal.krisztina@arany-alt.unideb.hu (R. Elian), kovacs.zsigmond@med.unideb.hu (Z.M. Kovács), szentandrassy.norbert@med.unideb.hu (N. Szentandrássy), martina.piga@ffa.uni-lj.si (M. Piga), tihomir.tomasic@ffa.uni-lj.si (T. Tomašič), nace.zidar@ffa.uni-lj.si (N. Zidar), veze@med.unideb.hu (Z. Varga).

https://doi.org/10.1016/j.biopha.2026.119530
Received 3 March 2026; Received in revised form 27 April 2026; Accepted 12 May 2026
Available online 20 May 2026

single protein containing four corresponding domains (DI-DIV) in Na_V and Ca_V channels. Each such subunit or domain is made up of six transmembrane helices (S1-S6) of which S1-S4 form the voltage-sensor domain (VSD) and S5 and S6 contribute to the pore domain. The S4 helix undergoes an outward motion upon membrane depolarization due to the presence of residues with positive side chains in every third position, termed gating charges. This outward movement couples to the pore domain resulting in channel opening and allowing ion permeation. A notable exception to this general structure is that of the voltage-gated proton channel, H_V1, which only consists of a VSD and lacks the pore for ion permeation [3,4]. Instead, very highly selective proton conduction is achieved via a continuous wire of water molecules and titratable residues of the VSD in its activated conformation [5]. The gating of H_V1 is dependent on the membrane potential and the transmembrane pH gradient, and the channel typically functions as a homodimer [6]. By regulating intracellular pH, it is involved in functions like reactive oxygen species production in immune cells, sperm cell capacitation and tumor cell migration [7–9].

Despite these similarities in voltage-sensing function, all these VGICs have unique physiological roles. Their widespread tissue distribution and essential physiological roles promoted VGICs to be attractive drug targets, and indeed, there are numerous currently used medications achieving their therapeutic effects via VGIC modulation. Well-known examples are lidocaine (local anesthetic), flecainide (antiarrhythmic) and phenytoin (anticonvulsant) acting on Na_V channels, nifedipine (antihypertensive) and ziconotide (analgesic) acting on Ca_V channels and amiodarone (antiarrhythmic) and 4-aminopyridine (for multiple sclerosis) acting on K_V channels [10–13]. Recently, the anti-arrhythmic agent ranolazine was even found to improve the survival of cancer patients, presumably via inhibiting the Na_V channels in cancer cells [14].

The mechanisms of action of these VGIC modulators show high variability. Channel function may be affected by a simple pore block or modification of gating, e.g. by shifting the voltage-dependence of activation or inactivation, VSDs can be trapped in various states and the binding affinity of the drug may also show state-dependence [15–17]. Functional selectivity, the affinity of a drug molecule depending on channel activity (relative times spent in various gating states), rather than structure-dependent isoform selectivity is an important aspect of drug development, especially in the case of the fast-gating Na_V channels.

Thus, many modulators of VGICs are known, yet, despite their

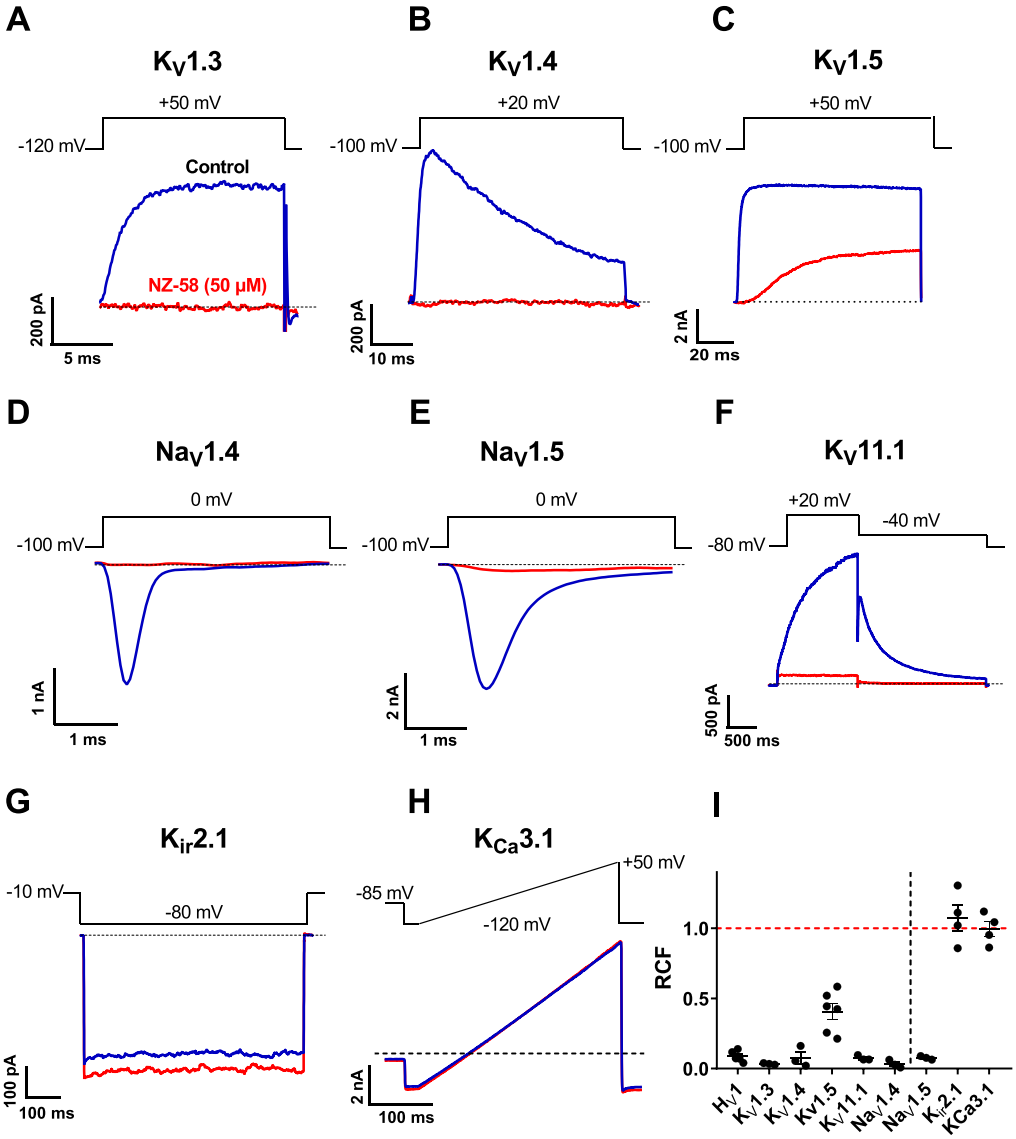

Fig. 1. Effect of 50 µM NZ-58 on voltage-gated and non-voltage gated ion channels. (A-H) NZ-58 was applied extracellularly in whole-cell patch clamp experiments. The currents were activated by the voltage protocols shown above the traces. Blue traces show the control, and red traces the inhibited currents. (I) The Remaining Current Fraction (RCF) is shown for each channel at 50 µM NZ-58, including H_V1 from our previous study. The red dashed line indicates the control current level.

proven utility and intense research, progress in this field has significantly slowed in the last few decades, as highlighted in the thorough review by Lopez Mateos et. al [11]. Very few potential drug candidates have reached clinical use despite intense research efforts and significant advances in automated electrophysiology screening techniques, protein structural information and computational methods. One main reason for this lack of success is that members of the K_V, Na_V and Ca_V families show high structural homology and functional similarity within the families, so developing isoform-selective molecules remains a significant challenge. On the other hand, considering the virtually endless number of potential blocking mechanisms and binding sites, molecules with novel modes of action offer new opportunities for developing such effective drugs.

Here, we describe an in-depth mode-of-action study for a molecule, named NZ-58 (*N*-(3-(2-amino-1*H*-imidazol-5-yl)phenyl)-5-(trifluoromethoxy)-1*H*-indole-2-carboxamide), which we published earlier ([18] labelled compound 13 in that study, Sup. Fig. 1) as an inhibitor of the H_V1 voltage-gated proton channel. However, further characterization revealed that NZ-58 acts as a "pan-VGIC" modulator, as it affected all voltage-gated ion channels tested, while showing no activity on non–voltage-gated ion channels. In addition, at concentrations below those required for full inhibition, it produced interesting kinetic changes in the ionic currents. For example, in the case of $Na_V1.5$, this resulted in channel activation rather than inhibition. $Na_V1.5$ is one of the nine isoforms of the voltage-gated Na^+ channel pore-forming alpha subunits, and is mainly expressed in cardiac myocytes, where it initiates the cardiac action potentials leading to contraction. Its gain-of-function and loss-of-function mutations can result in lethal arrhythmias like Long-QT and Brugada Syndromes, respectively.

In addition to $Na_V1.5$, we also performed a detailed characterization of the effects of NZ-58 on the $K_V1.3$ channel. $K_V1.3$ is the major cation channel of human lymphocytes and other immune cells, involved in membrane potential control and proliferation, and one of the earliest ion channels characterized by electrophysiology [19,20]. $K_V1.3$ lacks fast N-type inactivation, however, during sustained depolarization it inactivates via slow, C-type inactivation with a time constant of about 200 ms, which involves rearrangement of the selectivity filter region and is not directly linked to VSD movement [21–23].

$K_V1.3$ provides an interesting comparison with $Na_V1.5$ due to both structural and functional similarities, as well as key differences. They share a similar overall structure with four 4-transmembrane-helix VSDs, but while the VSDs are identical in both structure and function in the homotetrameric $K_V1.3$, the voltage-sensitivity, kinetics and functions of the VSDs in $Na_V1.5$ differ significantly. Notably, while the opening pathways are similar for the two channels relying on the activation of the VSDs [24], they inactivate by very distinct mechanisms. Unlike the selectivity-filter-linked slow C-type inactivation of $K_V1.3$, the fast, inactivation-motif-dependent inactivation of $Na_V1.5$ requires the activation of the Domain IV (D-IV) VSD [25]. Moreover, the relative rates of activation and inactivation also differ significantly.

Highlighting the similarities and differences in the actions of NZ-58 on these channels, we describe its unique modes of modulation and propose that despite its lack of selectivity, it may offer new pathways to explore in the drug design for VGICs.

2. Materials and methods

2.1. Cell culture and preparation

Chinese hamster ovary (CHO) cells were cultured as described previously [26]. Cells were maintained in Dulbecco's Modified Eagle Medium (DMEM; Gibco, Thermo Fisher Scientific, Waltham, MA, USA, Cat# 11965084) supplemented with 10% fetal bovine serum (FBS; Sigma-Aldrich), 2 mM L-glutamine, 100 μg/mL streptomycin, and 100 U/mL penicillin-G (Sigma-Aldrich, St. Louis, MO, USA). Cultures were kept at 37 °C in a humidified atmosphere of 5% CO_2 and 95% air. Cells were passaged twice weekly following a 2–3 min incubation in PBS containing 0.2 g/L EDTA (Invitrogen, Waltham, MA, USA). The ion channel constructs used in this study were obtained from the following sources: $hK_V1.4$-IR, the inactivation ball deletion mutant of $K_V1.4$ (a gift from D. Fedida, University of British Columbia, Vancouver, Canada); $hK_V1.5$ in the pRcTAL C1 YFP plasmid (a gift from A. Felipe, University of Barcelona, Spain); $hK_V11.1$ (a gift from H. Wulff, University of California, Davis, USA); $hNa_V1.5$ in pH1TO-EGFP plasmid and $hNa_V1.4$ (gifts from P. Lukács, Eötvös Loránd University, Budapest, Hungary); $mK_{ir}2.1$ in CMV pA CMV mRFP pA AV39 plasmid (a gift from I. Levitan, University of Illinois, Chicago, USA); and $hK_{Ca}3.1$ in the pCMV6 AC GFP plasmid (a gift from B. Attali, Tel Aviv University, Israel). CHO cells were transiently transfected using a Lipofectamine 2000 kit (Invitrogen, Carlsbad, CA, USA) as per the manufacturer's protocol with the above ion channel coding vectors. $hK_V1.4$ was transiently co-transfected with a plasmid encoding the green fluorescent protein (GFP) at a molar ratio of 10:1. For the $K_V11.1$ and $Na_V1.4$ currents were recorded from stably expressing HEK cell lines.

Human peripheral blood mononuclear cells (PBMCs) were isolated from venous blood obtained from anonymized healthy donors as described earlier [27]. Blood samples were collected by having approval from the Ethical Committee of the Hungarian Medical Research Council (36255–6/2017/EKU). PBMCs were isolated by Histopaque1077 (Sigma-Aldrich Hungary, Budapest, Hungary) density gradient centrifugation. The isolated cells were resuspended in Roswell Park Memorial Institute (RPMI) 1640 medium (Gibco, Cat# 11875085) supplemented with 10% fetal calf serum (FCS, Sigma-Aldrich, St. Louis, MO, USA), 100 μg/mL penicillin, 100 μg/mL streptomycin, and 2 mM L-glutamine. They were then seeded into 24-well culture plates at a density of 5–6 × 10^5 cells/mL and maintained in a 5% CO_2 incubator at 37 °C for 3–5 days. Phytohemagglutinin A (PHA, Sigma-Aldrich, St. Louis, MO, USA) was added at 8–12 μg/mL to enhance $K_V1.3$ expression. Most measurements on $K_V1.3$ were performed on PBMCs, but the mutant channels and the inside-out experiments requiring high channel expression were performed on transfected CHO cells.

CHO cells, PBMCs, and HEK cells were gently washed twice with 2 mL of extracellular solution, used for patch-clamp experiments, and replated onto 35-mm polystyrene culture dishes (Cellstar, Greiner Bio-One, Kremsmünster, Austria). GFP-positive transfected cells were identified using a Nikon TS100 fluorescence microscope (Nikon, Tokyo, Japan) with 455–495 nm excitation and 515–555 nm emission filters. In general, ionic currents were recorded 24–36 h after transfection, whereas $hK_V1.3$ currents were measured in activated lymphocytes 4–5 days after stimulation.

2.2. Mutagenesis

R373C and R367C mutations were introduced into the pC1-EGFP-hKv1.3-WT and the R1632C into the pH1TO-EGFP-Nav1.5 plasmids, respectively. For Kv1.3, the two sets of mutagenesis primers were designed following the one-step site-directed mutagenesis protocol of Liu et al. [28]. The primers were designed with an overlapping 5' region and a non-overlapping 3' extension (Integrated DNA Technologies-IDT, Leuven, Belgium). PfuUltra II polymerase was used (Agilent Technologies, Santa Clara, CA, USA), as well as dNTPs, *Dpn*I enzyme (Thermo Fisher Scientific, Waltham, MA, USA). For Nav1.5, two-sets of primers were designed, the overlapping mutagenesis primers and the flanking primers containing restriction sites at the 5' and 3' ends of the mutation site. FastDigest (FD) enzymes (FD-*Kpn*I & FD-*Xho*I) (Thermo Fischer Scientific, Waltham, MA, USA) were used, the digested products were extracted from the gel using QIAquick gel extraction kit (Qiagen, Germany), then ligated in a 3:1 molar ratio using Rapid ligation kit (Thermo Fischer Scientific, Waltham, MA, USA). The ligated constructs were transformed into chemically competent *E. coli* Top10F'. All the mutants and wild-type constructs were confirmed by DNA sequencing (Plasmidsaurus, Louisville, KY, United States) before electrophysiological

experiments.

2.3. Electrophysiology

Using voltage-clamp mode, the standard whole-cell patch clamp configuration or inside-out configuration were used to record ionic currents as described previously [26]. Micropipettes were pulled in four stages using a Flaming Brown automatic pipette puller (Sutter Instruments, San Rafael, CA, USA) from GC 150F-15 borosilicate glass capillaries (Harvard Apparatus Co., Holliston, MA, USA) with tip diameters between 0.5 and 1 μm and a tip resistance ranging typically between 3 and 5 MΩ. All measurements were carried out using Axopatch 200B amplifiers connected to personal computers using Digidata 1550B data acquisition hardware (Molecular Devices Inc., Sunnyvale, CA, USA). Records were discarded when the leak at the holding potential exceeded more than 10% of the peak current at the given test potential. Experiments were conducted at room temperature, which ranged between 20 and 24 °C.

For measuring Na_V currents, the holding potential was –100 mV, and depolarizing pulses to 0 mV with durations ranging from 15 to 50 ms were delivered at 5-s intervals unless otherwise specified. For $K_V1.3$, 15–2000-ms-long depolarizations to + 50 mV were used from a holding potential of −100 mV with interpulse intervals of 15–60 s. Recordings of $K_V1.5$ currents were obtained using 100-ms depolarizing steps to 50 mV, applied every 15 s from a holding potential of –100 mV. For the measurement of $K_V1.4$, we used a 50 ms step protocol from a holding potential of −100 mV to + 20 mV. The $K_V11.1$ current was recorded using a voltage-step protocol consisting of a holding potential of –80 mV, followed by a 1250-ms depolarizing pulse to + 20 mV, and subsequently a 2-s hyperpolarizing step to –40 mV delivered every 30 s. Peak tail currents were quantified during the hyperpolarizing step. For $K_{Ca}3.1$ currents, a 200-ms-long voltage ramp to + 50 mV from –120 mV was applied every 10 s. The $K_{ir}2.1$ current was measured using a 600-ms voltage-step protocol, applying steps from a holding potential of –10 mV to –80 mV.

2.4. Solutions

Solutions were freshly prepared, pH checked before patch clamp recordings and osmolarities of the extracellular solution (ECS) and intracellular solution (ICS) were measured between 302 and 308 mOsm/L and ~295 mOsm/L, respectively. For $hK_V1.3$, $hK_V1.4$, $hK_V1.5$, $hK_V11.1$, $hNa_V1.4$, and $hNa_V1.5$, the ECS (bath) contained 145 mM NaCl, 5 mM KCl, 2.5 mM $CaCl_2$, 1 mM $MgCl_2$, 10 mM Hepes, and 5.5 mM glucose (pH = 7.35 titrated with NaOH), and the ICS (pipette) for K_V channels contained 140 mM KF, 2 mM $MgCl_2$, 1 mM $CaCl_2$, 11 mM EGTA, and 10 mM Hepes (pH = 7.2 with KOH) [26]. For potassium channels, a high K^+-based ECS was used as an indicator of the proper solution exchange, whose composition was identical to standard ECS except that it contained 150 mM KCl and 0 mM NaCl. For Na_V current recordings, Cs^+-based ICS was used to avoid the recordings of endogenous K^+ currents; thus, the ICS consisted of (in mM) 10 NaCl, 105 CsF, 10 HEPES, and 10 EGTA (pH = 7.2 titrated with CsOH). For the $K_{ir}2.1$ measurements, the extra and intracellular solution consisted of (in mM) 72.5 NaCl, 77.5 KCl, 2.5 $CaCl_2$, 1 $MgCl_2$, 10 HEPES, and 5.5 glucose (pH = 7.35 titrated with KOH) and 140 KF, 2 $MgCl_2$, 1 $CaCl_2$, 11 EGTA, 1 Na-ATP and 10 HEPES (pH = 7.2 with KOH). For $hK_{Ca}3.1$, the ECS contained 145 mM L-aspartic acid with Na, 5 mM KCl, 2.5 mM $CaCl_2$, 1 mM $MgCl_2$, 10 mM Hepes, and 5.5 mM glucose (pH = 7.4 with NaOH), and the ICS contained 145 mM K-Asp, 2 mM $MgCl_2$, 8.5 mM $CaCl_2$, 10 mM EGTA, and 10 mM Hepes (pH = 7.2 with KOH), giving ~2 μM free Ca^{2+} to fully activate the $hK_{Ca}3.1$ current. For Na_V channels, a choline-based ECS was used for perfusion control, whose composition was (in mM) 145 choline-Cl, 5 KCl, 10 HEPES, 5.5 glucose, 2.5 $CaCl_2$, and 1 $MgCl_2$. The same ECS was used for gating current measurements to avoid the interference from endogenous Na_V channels in CHO cells. Bath perfusion around the measured cell with different extracellular solutions was achieved using a gravity flow micro perfusion system at a rate of 200 μL/min. Excess fluid was removed continuously. NZ58 solutions were made fresh in ECS from 10 or 20 mM stocks stored at −20 °C. Stock solutions were prepared from powder dissolved in water-free DMSO (Sigma-Aldrich, Budapest, Hungary).

As 10 μM NZ-58 produced significant gating changes, we aimed at performing all measurements at this concentration. However, protocols lasting over several minutes (especially in the case of $K_V1.3$), or after multiple rounds of compound application and washout, irreversible changes occurred, which distorted the data. In these cases, we applied shortened protocols by reducing the number of recorded sweeps and / or performed the experiments with 5 μM concentration. This concentration still produced significant changes, so the obtained results are relevant and comparable with the 10 μM data.

2.5. Patch clamp data analysis

The pClamp 10.7 software package (Molecular Devices Inc., Sunnyvale, CA, USA) and GraphPad Prism 8 (GraphPad, CA, USA) were used for data acquisition and analysis. In general, currents were lowpass-filtered using the built-in analog four-pole Bessel filters of the amplifiers and were sampled (2–50 kHz) at least twice the filter cut-off frequency. Before analysis, current traces were digitally filtered with a Gaussian filter and were corrected for ohmic leakage when needed [26].

The inhibitory effect of the drug at a given concentration was calculated as remaining current fraction ($RCF = I/I_0$, where I_0 is the peak current in the absence of the drug, and I is the peak current at equilibrium block at a given drug concentration). Fitting of data points was performed as described earlier [29]. The activation kinetics and recovery from inactivation were fitted by a standard single rising exponential function: $= A \times (1 - \exp(-K \times x)) + C$, while inactivation kinetics with a decaying exponential: $Y = A \times \exp(-K \times x) + C$, from which the time constants were obtained ($\tau = 1/K$).

For the steady-state activation G-V curves, the peak conductance (G) at each test potential was calculated from the peak current (I) measured at the given membrane potential (E_m) and the reversal potential (E_{rev}) using the chord-conductance equation: $G = I/(E_m - E_{rev})$. Normalized conductance (G_{norm}) was obtained by dividing each conductance value by the maximal conductance across all test potentials. For steady-state inactivation, the peak current during the depolarizing pulses were recorded after keeping the cell at increasing holding potentials. The measured current amplitudes were normalized to the peak measured at the most negative membrane potential. The resulting G_{norm} and I_{norm} values, representing the voltage dependence of steady-state activation and inactivation, were plotted as functions of the membrane potential. Quantification was performed by fitting the data with Boltzmann functions $G_{norm} = 1/(1 + \exp((V_{50} - V_m)/k))$ and/or $I_{norm} = 1/(1 + \exp((V_m - V_{50})/k))$ respectively where V_{50} is the half-activation voltage and k is the slope factor.

Data are given as mean ± SEM, for a minimum of 3 independent experiments. In most cases, values were obtained on the same cell before and after treatment, so a paired *t*-test was used. For ratio comparisons, a one-sample *t*-test was used with a theoretical mean of 1. For independent samples, 2-sample *t*-tests or one-way ANOVA were used. A change was deemed significant at $p < 0.05$.

3. Results

3.1. NZ-58 is a pan-VSD modulator

We have previously described NZ-58 as a potent inhibitor of the H_V1 proton channel (IC_{50} = 8.5 μM, [18]), which not only inhibited the proton current but also affected the voltage-dependent gating of the channel (Feher et al., under review). Both the opening threshold voltage and the opening and closing kinetics were accelerated by NZ-58 binding

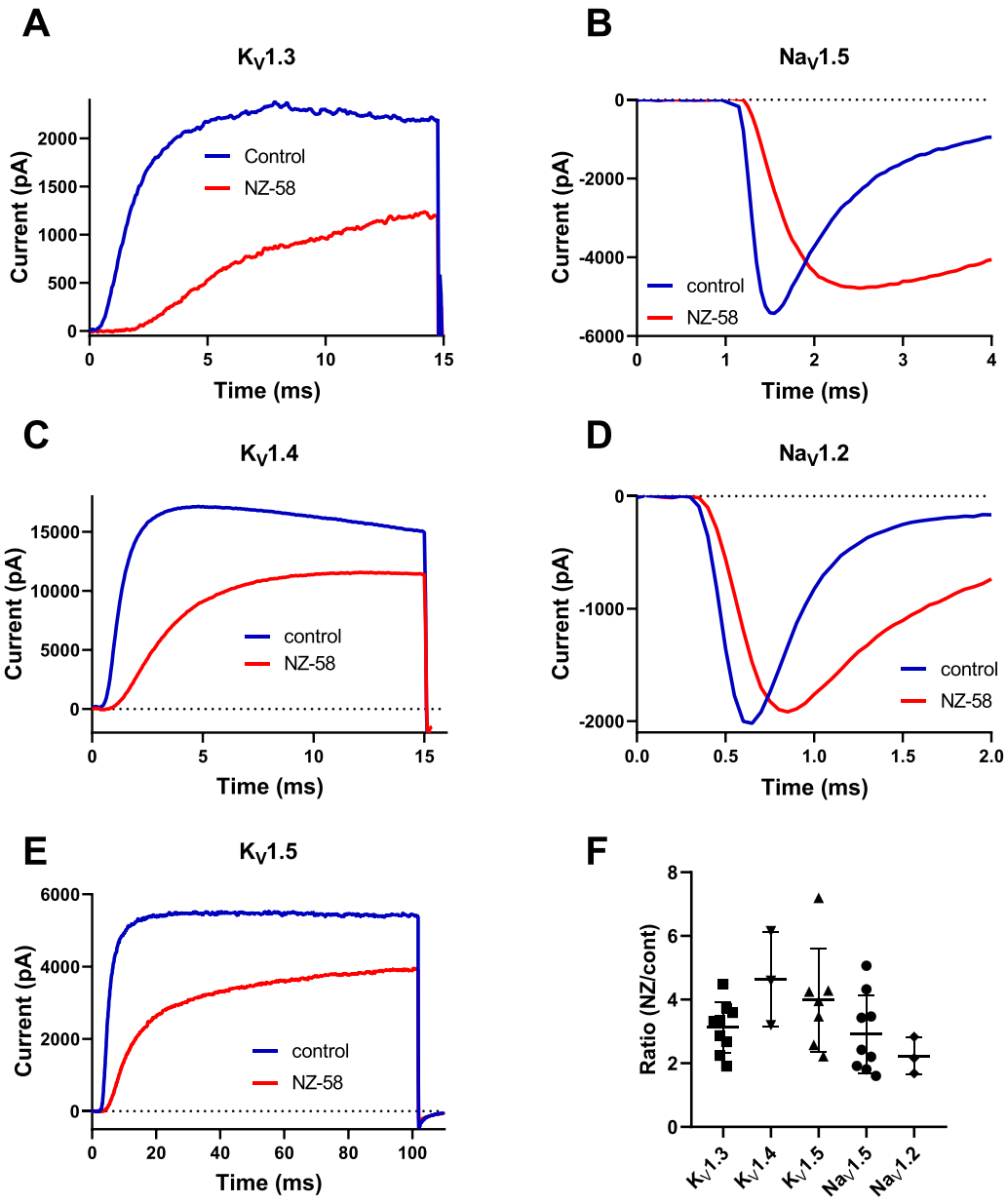

Fig. 2. Effect of 10 μM NZ-58 on the activation kinetics of K_V and Na_V channels. (A-E) Drastic slowing of current activation kinetics of the indicated ion channels in response to NZ-58. Currents were elicited by depolarizing pulses to + 50 mV for K_V channels and to 0 mV for Na_V channels. (F) Summary of the changes induced in the activation time constants expressed as the ratio in the presence and absence of the compound.

(Sup. Fig. 2.). In order to assess the selectivity of the compound, we evaluated its effect by whole-cell patch clamp on multiple ion channels, including VGICs Na_V1.5, Na_V1.2, Na_V1.4, K_V1.3, fast inactivation-removed K_V1.4, K_V1.5, K_V11.1 (hERG), as well as the non-voltage-gated K_{ir}2.1 and K_{Ca}3.1 channels. These initial experiments were performed with extracellular application of 50 μM NZ-58, which caused nearly complete inhibition of the currents of all VGICs tested, with the exception of the non-inactivating K_V1.5. In contrast, NZ-58 but had no detectable effect on the currents mediated by the non-VGICs

As 50 μM NZ-58 almost completely suppressed the currents, preventing the assessment of potential effects on channel gating, we applied it at lower concentrations as well. At 10 μM (close to the IC_{50} on H_V1), NZ-58 caused significant gating changes in VGICs with only a small current reduction in most channels. The observed effects were variable throughout the channels with some common features and some more channel-specific and opposing effects.

The most notable effect on all K_V1.x and Na_V1.x channels was the robust slowing of activation kinetics (Fig. 2A-2E). This was assessed by single exponential fits for easier comparison, although, due to the multi-VSD nature of current activation, the rise of the current traces was often clearly sigmoidal. Fig. 2F shows the dramatic slowing of current activation by 10 μM NZ-58 in some VGICs, expressed as the ratio of the activation time constants in the presence and absence of the compound. This suggests a direct interaction of NZ-58 with the VSDs, which was further supported by the lack of effect on non-VGICs K_{ir}2.1 and K_{Ca}3.1 (Fig. 1G and H).

Slowing of VSD activation may indicate a process stabilizing the resting state and thus slowing of the forward rate and speeding of the backward rate, which should manifest as faster deactivation (channel closing) at negative potentials. Although NZ-58 had a complex effect on H_V1 activation kinetics, resulting in an overall acceleration, it also significantly increased the rate of channel closing (Sup. Fig. 1, Feher et al., under review). In order to assess the effect of NZ-58 on the channel closing rate of other VGICs, we measured tail current kinetics in K_V1.3

and $Na_V1.5$ channels. For this, we stepped back to negative membrane potentials following a depolarizing pulse that opened most of the channels and fitted the recorded the decaying traces with exponential functions. Unlike in H_V1, we observed no change in the tail current kinetics of $K_V1.3$ or $Na_V1.5$ channels ($K_V1.3$: control: 6.28 ± 0.50 ms, NZ-58: 6.78 ± 0.86 ms, n = 4, p = 0.89; $Na_V1.5$: control: 0.199 ± 0.059 ms, NZ-58: 0.168 ± 0.044 ms, n = 4, p = 0.86; Fig. 3). Since the rate of deactivation of $Na_V1.5$ at −100 mV was comparable to the clamping speed, tail kinetics was measured at −70 mV, which made it significantly slower and therefore reliable for comparison. This implies a mechanism distinct from that on H_V1, in which only the activation energy of the rate-limiting forward transition is increased, while that of the backward transition remains unaffected.

3.2. *Effects on wild type $Na_V1.5$*

A remarkable effect of NZ-58 on Na_V channels (studied here in detail on $Na_V1.5$) was a significant slowing of fast inactivation along with activation (Fig. 4A). 10 μM NZ-58 induced kinetic changes on $Na_V1.5$ within a few seconds without much effect on the current amplitude, but the full effect developed over the course of a few minutes. As the relative rates of activation and inactivation determine the current amplitude and the amount of charge transferred through the channels (area under the current trace), which ultimately defines the activator or inhibitor nature of the compound, we investigated the dose-dependence of the kinetic changes. Lower concentrations resulted in a significant increase in the total charge transfer during the depolarizing pulse (Fig. 4A), corresponding to an activating effect, which had a dose-dependence on the amplitude and the charge transferred as shown in Fig. 4B and C. At 10 μM the amplitude was barely reduced but the charge transfer almost tripled compared to the control trace. High concentrations (25 and 50 μM) induced a quick temporary increase in the charge passed, but within a few minutes this value declined, in the case of 50 μM even below the control value.

These variable changes may be explained by the different rates at which activation and inactivation kinetics were altered. As shown in Fig. 5, initially, the inactivation rate slows more than the activation rate, which can result even in a slight amplitude increase accompanied by increased charge passage. However, with time, the slowing of inactivation seems to slow and saturate, while the activation keeps getting slower resulting in amplitude reduction and, in the case of high concentrations, charge transfer reduction. Fig. 5B clearly shows a sigmoid time course for the slowing of the activation kinetics due to the requirement of the activation of three VSDs for channel opening. For a direct comparison, however, we fit both time courses with a single exponential function, whose time constants clearly reveal the slower overall change in the activation kinetics (τ_{act} = 82.7 ± 10.3, τ_{inact} = 41.3 ± 5.0, n = 5, p = 0.009). As the association rate of the compound is proportional to the concentration, 50 μM NZ-58 quickly and dramatically slows activation to nearly completely suppress the current amplitude and the charge transfer. Following short-term application of low concentrations, the effects were fully reversible, however, application over several minutes or repeated applications, especially with higher concentrations, resulted in irreversible kinetic changes.

Besides altering the activation energy barrier between conformational states, small molecule modulators may also change the energy difference between the states. Therefore, we checked the voltage-dependence of steady-state activation (G-V) and inactivation (SSI) of $Na_V1.5$ in the presence of NZ-58. We obtained current – voltage (I-V) relationships and constructed normalized conductance - voltage (G-V) relationships. For the SSI curves, the fraction of available channels was assessed by depolarizing pulses from various holding potentials. Surprisingly, neither function was affected by the compound implying that the energetics between the resting and activated states of the VSDs were unaffected (G-V: $V_{0.5,cont}$ = −36.0 ± 3.4 mV, $V_{0.5,NZ}$ =-32.8 ± 4.1 mV, p = 0.16; SSI: $V_{0.5,cont}$ = −69.6 ± 1.0 mV, $V_{0.5,NZ}$ =-70.1 ± 2.1 mV, p = 0.70; Fig. 6).

As the rate of fast inactivation was strongly affected by NZ-58, we hypothesized that it may also influence the rate of the recovery from inactivation and the extent of cumulative inactivation during high frequency pulsing. Indeed, the recovery from inactivation was significantly hindered by the compound (Fig. 7A, τ_{cont} = 10.9 ± 1.9 ms, τ_{NZ} = 18.4 ± 2.3 ms, n = 4, p = 0.001). Consequently, cumulative inactivation during high frequency stimulation (200 ms-long depolarizations at 3 Hz, corresponding to a 180 bpm heart rate) was also significantly enhanced, as evidenced by the faster decrease of subsequent current amplitudes and the lower remaining current fraction in the presence of NZ-58 (Fig. 7B, Remaining current fractions: 0.47 ± 0.10 for control, and 0.14 ± 0.06 for 10 μM NZ-58, n = 3) (Fig. 8).

NZ-58 presumably binds directly to the VSDs, whose external accessibility may depend on the gating state of the channels, being more deeply buried in the resting state and more exposed in the activated state. We therefore tested whether NZ-58 could bind the channels when they were kept in the closed state at a negative membrane potential. After recording a control trace, we applied the compound for 20 s at −100 mV, then switched back to the control solution before recording the current and assessing its effect. We found that NZ-58 induced the same changes during closed state application as during continuous pulsing, indicating the state-independent binding (Fig. 7C).

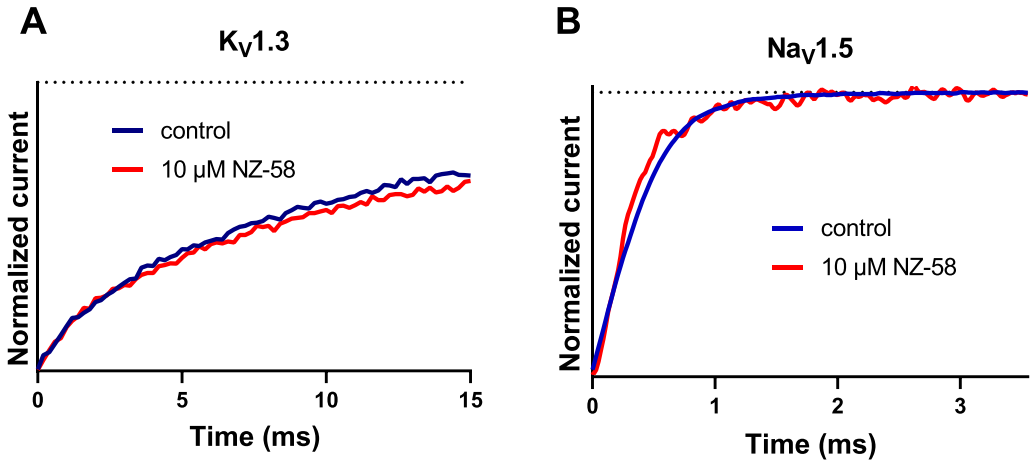

Fig. 3. Effect of NZ-58 on the tail currents of $K_V1.3$ and $Na_V1.5$ channels. Tail currents were measured at −100 mV after stepping back from + 50 mV with $K_v1.3$ or at −70 mV returning from 0 mV with $Na_V1.5$ before significant inactivation occurred during the depolarizing pulse.

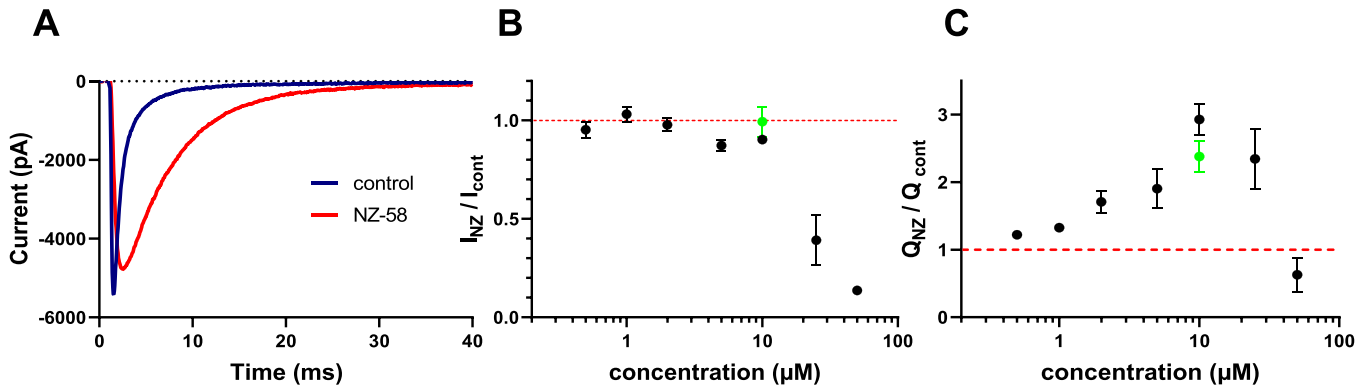

Fig. 4. The effect of NZ-58 on the kinetics and charge transfer of $Na_V1.5$ channels. (A) Application of 10 μM NZ-58 induced significant slowing of both the activation and inactivation kinetics, increasing total charge transfer. (B) Changes in the current amplitude as a function of NZ-58 concentration. Black symbols represent the wild type channel, the green symbol represents the R1632C mutant channel (see below). The red dashed line represents the control value. (C) Total charge transferred (area under the current trace) as a function of concentration. For the various concentrations n = 3–8.

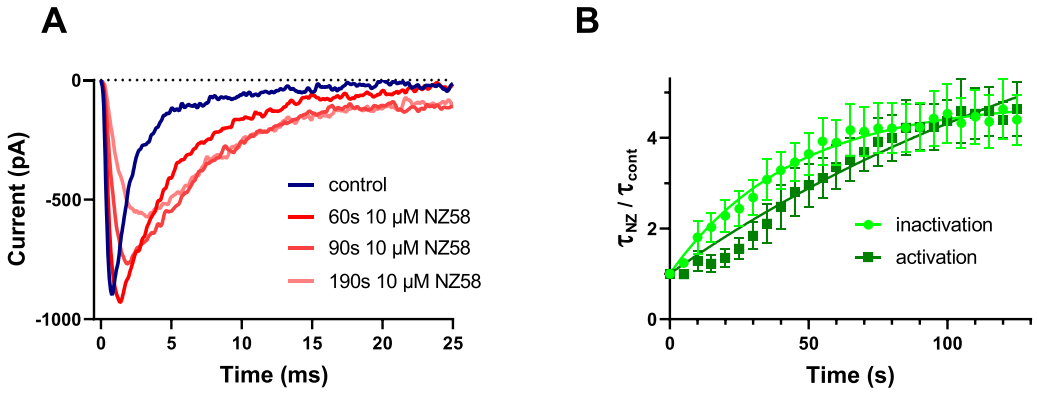

Fig. 5. Changes in $Na_V1.5$ activation and inactivation kinetics with time. (A) Development of the current traces as a function of time following the application of 10 μM NZ-58. (B) The change of the ratio of the activation and inactivation time constants compared to control as a function of time. Points represent the average ratios for n = 5 cells. Although the slowing of the activation kinetics clearly shows a sigmoid time course due to the three VSDs required for activation, both datasets were fit with single exponentials for easier comparison of the time courses.

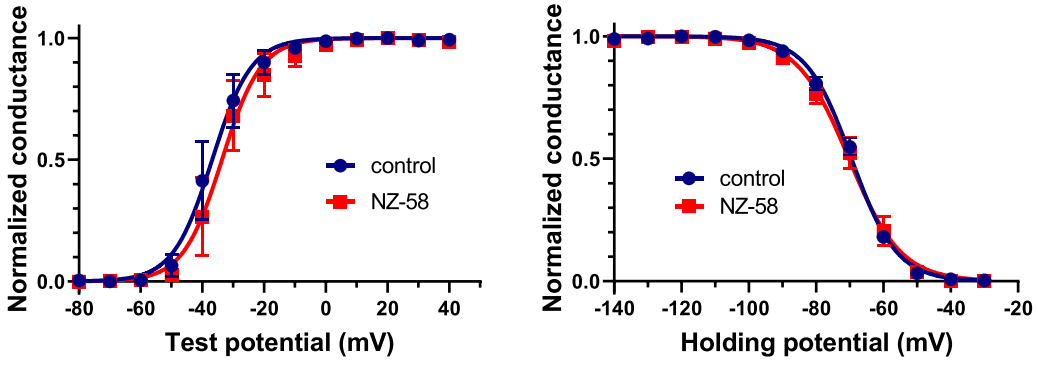

Fig. 6. Voltage-dependence of steady-state activation and inactivation of $Na_V1.5$. (A) G-V curves were constructed from I-V relationships using increasing step depolarizations in the absence and presence of 5 μM NZ-58. (B) Depolarizations to 0 mV were used to determine the fraction of available channels at various holding potentials. Blue symbols: control, red symbols: 5 μM NZ-58.

3.3. The Brugada mutant $Na_V1.5$-R1632C

The similarly drastic slowing of voltage-gated opening on the tested voltage-gated channels and the lack of effect on the non-voltage gated ones, suggested that NZ-58 likely binds to a region in the VSDs conserved across these channels. Sequence comparison did not reveal common segments other than the highly conserved signature positive gating charges (mostly arginines) in every third position. Assuming that these residues may be influential for binding, we mutated the 4th arginine (R4) in the DIV-VSD of $Na_V1.5$ and generated the R1632C mutation as it is a known loss-of-function Brugada mutant [30]. We could confirm the published properties of the mutant channel such as reduced expression, significantly left-shifted steady-state inactivation curve, and extremely slow recovery from inactivation (Sup. Fig. 3), and then tested the affinity of the mutant for the compound. The mutation had no significant effect on the affinity of NZ-58, as it induced the same kinetic

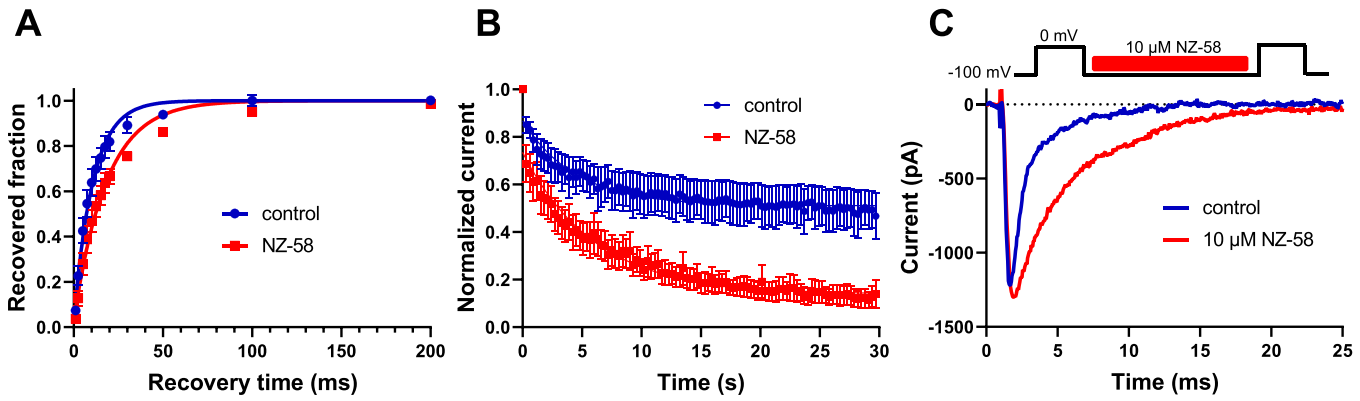

Fig. 7. Recovery from inactivation, cumulative inactivation and closed state binding in $Na_V1.5$. (A) Recovery from inactivation was measured by pulse pairs separated by increasing recovery periods at −100 mV. The fraction of recovered channels is plotted as a function of recovery time. Blue: control, red: 5 μM NZ-58. (B) Cumulative inactivation was assessed by delivering 200 ms-long pulses to 0 mV at 3 Hz. Normalized current amplitudes are plotted as a function of time. (C) A control trace (blue) was recorded, then 10 μM NZ-58 was applied for 20 s while keeping the channels closed at −100 mV, followed by a switch back to control solution and the recording of the second trace (red). Kinetic changes indicate closed state binding.

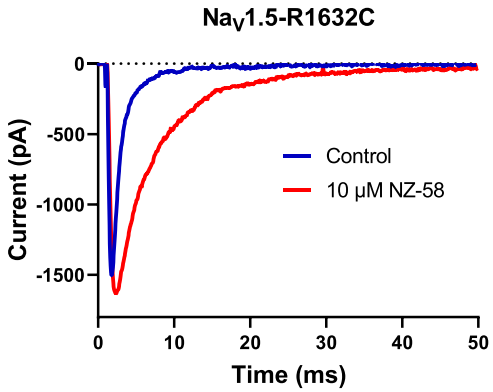

Fig. 8. Effect of NZ-58 on the Brugada-mutant $Na_V1.5$-R1632C. Application of 10 μM NZ-58 induced similar kinetic changes in the mutant channel as in the wild type.

changes as in the wild type channel, and neither the effect on the current amplitude nor on the charge transfer was different between the two channels (Figs. 4B and 4C, green symbols, amplitude ratio: WT: 0.90 ± 0.02, n = 8; mutant: 0.99 ± 0.08, n = 9, p = 0.29; charge transfer ratio: WT: 2.93 ± 0.24, mutant: 2.38 ± 0.23, p = 0.12).

3.4. *Effects on $K_V1.3$*

Motivated by the similar slowing of VSD movement by NZ-58 in various VGICs, we decided to investigate the effects on $K_V1.3$, a representative of the voltage-gated K^+ channel family in more detail. The objective of these experiments was the comparison of the effects on $K_V1.3$ versus $Na_V1.5$, as the two channels have both similar and distinct gating features. As mentioned above, 10 μM NZ-58 drastically slowed $K_V1.3$ channel opening kinetics ($\tau_{act,NZ}$ / $\tau_{act,cont}$ = 3.13 ± 0.27, n = 9, p < 0.001), but surprisingly it did not affect the rate of channel closing at all ($\tau_{deact,NZ}$ / $\tau_{deact,cont}$ = 1.03 ± 0.13, n = 8, p = 0.82; Figs. 2A and 3A). This agrees with the observations made on $Na_V1.5$. However, in stark contrast with $Na_V1.5$, where fast inactivation is linked to DIV-VSD

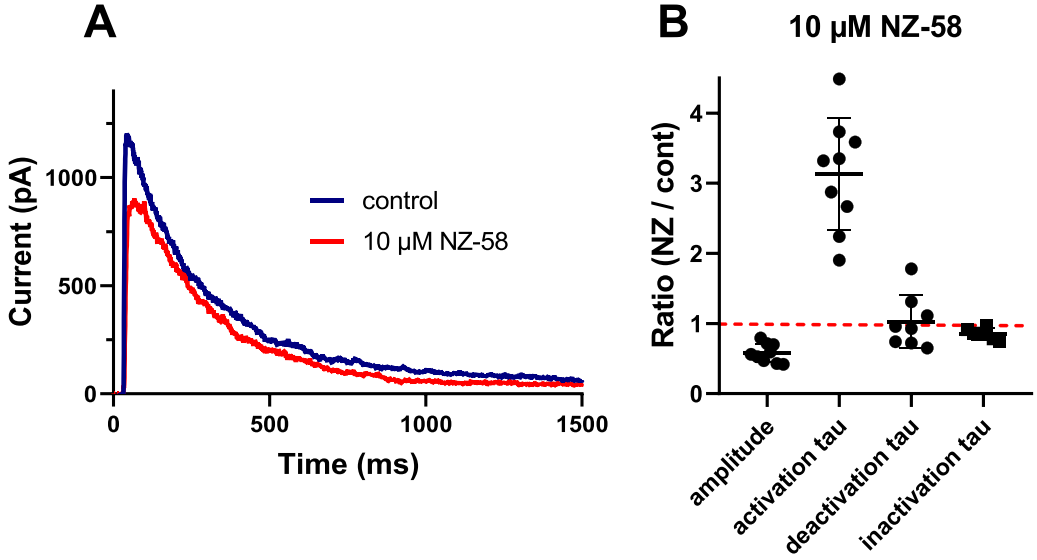

Fig. 9. Effects on current amplitude and gating kinetics of $K_V1.3$. (A) NZ-58 slows activation kinetics and slightly speeds C-type inactivation, which result in a reduction of the current amplitude. Currents were recorded from a human lymphocyte by depolarizations to + 50 mV. (B) Changes induced in the current amplitude, current activation, deactivation and inactivation time constants by 10 μM NZ-58 expressed as the ratio of the parameters measured in the presence to those in the absence of the compound. The red dashed line represents the reference control value.

movement, the non-VSD-linked slow, C-type inactivation of $K_V1.3$ was weakly and oppositely affected, which manifested as a slight speeding of inactivation ($\tau_{inact,NZ}$ / $\tau_{inact,cont}$ = 0.86 ± 0.03, n = 6, p = 0.006; Fig. 9.). The concomitant slowing of activation and speeding of inactivation kinetics resulted in current amplitude reduction (at 10 μM: I_{NZ} / I_{cont} = 0.58 ± 0.04, n = 9, p < 0.001; Fig. 9), which at 50 μM culminated in complete current block (Fig. 1A). It should be noted that application of NZ-58 at 50 μM for more than 2–3 min resulted in the loss of the patch configuration and even at 10 μM, application beyond 7–8 min resulted in irreversible kinetic changes and current rundown.

The strong effect on the VSD motion implies that other aspects of voltage-dependent gating may be altered by NZ-58 binding, so similarly to $Na_V1.5$, we examined whether the compound affects the voltage-dependence of steady-state activation. Due to the strong activation-slowing effect of NZ-58, the usual protocol had to be extended to be able to detect the peak amplitude during intermediate depolarizing pulses. Interestingly, we observed only a slight, non-significant right-shift in the G-V relationship induced by 10 μM NZ-58 (Fig. 10A; $V_{0.5,cont}$ = −11.4 ± 2.5 mV, $V_{0.5,NZ}$ = −6.3 ± 3.7 mV, n = 7, p = 0.15). Furthermore, the markedly slower activation reduces current amplitude, which is more significant at lower voltages accompanied by slower activation rates, and this can cause an apparent right-shift. Considering this, the change in the voltage-dependence of activation is negligible. As for $Na_V1.5$, we assessed the voltage-dependence of steady-state inactivation, albeit with a shortened protocol. This was necessary due to the slow recovery from inactivation of $K_V1.3$ (τ_{rec} ≈ 15 s) requiring long inter-pulse intervals, which result in lengthy protocols, during which slow irreversible effects of the compound and current rundown can introduce artefacts. Our results showed no significant shift in the $V_{0.5}$ induced by NZ-58 (Fig. 10B; $V_{0.5,cont}$ = −43.6 ± 0.8 mV, $V_{0.5,NZ}$ = −43.7 ± 0.5 mV, n = 4, p = 0.92).

Since the steady-state inactivation was unaffected and the rate of inactivation was only slightly altered, we hypothesized that unlike in $Na_V1.5$ the rate of recovery from inactivation would be unaffected. The recovery from inactivation was assessed by a double pulse protocol, but also reduced to three pulse pairs due to the long duration of the full protocol, and NZ-58 was applied at 5 μM to avoid long-term rundown effects. Time constants were extracted from single exponential fits to the data points. As expected, unlike in $Na_V1.5$, NZ-58 had no effect on the recovery rate of $K_V1.3$ (Fig. 10C; τ_c = 14.44 ± 0.78 s, τ_{NZ} = 14.98 ± 0.77 s, p = 0.71, n = 3).

Similarly to $Na_V1.5$, we intended to test the potential interactions of NZ-58 with the gating arginines in $K_V1.3$. We therefore generated the $K_V1.3$ R367C (R2) and R373C (R4) mutants, and tested the efficacy of the compound on them. While the induced effects at 10 μM were qualitatively similar, the slowing in the activation kinetics and consequently the amplitude reduction were more robust in the mutants than in the wild type (activation tau ratios: WT: 3.1 ± 0.3, R367C: 10.6 ± 2.5, R373C: 16.5 ± 3.6, ANOVA: p = 0.002; amplitude ratios: WT: 0.58 ± 0.04, R367C: 0.23 ± 0.06, R373C: 0.41 ± 0.11, ANOVA: p = 0.0036).

Although we observed the effects described above when NZ-58 was applied extracellularly, considering its lipophilic nature (logD > 4.56, [31]), we assumed that it would be able to dissolve into and cross the plasma membrane. We therefore examined the sidedness of channel accessibility [32]. We performed inside-out patch experiments on $K_V1.3$ channels expressed in CHO cells and applied the compound from the intracellular side of the membrane. We observed identical effects to those seen with extracellular application, confirming access of NZ-58 to the binding site from the intracellular side as well (Figs. 11–13A).

3.5. Gating current measurements

While the above results suggest a direct effect of NZ-58 on the VSD movements, other potential explanations also exist. Slow current activation may be the result of the compound slowing the final pore-opening transition or altering the communication between the VSD and the pore. In order to investigate these alternatives, we carried out gating current measurements with the non-conducting W384F mutant of $K_V1.3$. In the absence of ionic current through the pore, these measurements directly report on gating charge movement originating from the displacement of the VSDs. Application of 10 μM NZ-58 significantly slowed the ON gating currents produced by the activation of the VSDs during depolarization, but surprisingly, no such effect could be observed on the OFF gating currents produced by the return of the VSDs to the resting state upon repolarization (Fig. 12B). This is in accordance with the effects observed on the ionic currents, where channel opening was significantly slowed by NZ-58 in both Na_V and K_V channels, but channel closing was not. The ON and OFF gating charges were equal in the presence of NZ-58 (Q_{OFF} / Q_{ON} = 0.960 ± 0.020, n = 7, p = 0.095), indicating the lack of charge immobilization. In addition, the total integrated gating charge did not significantly change upon the application of the compound ($Q_{ON,NZ}$ / $Q_{ON,cont}$ = 1.05 ± 0.04, n = 7, p = 0.26), implying that the VSDs complete the entire activation trajectory, only at a slower rate. By increasing step depolarizations, we attempted to acquire Q-V relationships, which measure the amount of gating charge displaced at the given membrane potential. However, the extremely slow VSD activation in the presence of NZ-58 at intermediate voltages prevented accurate charge integration suitable for statistical comparison of the $V_{0.5}$ values.

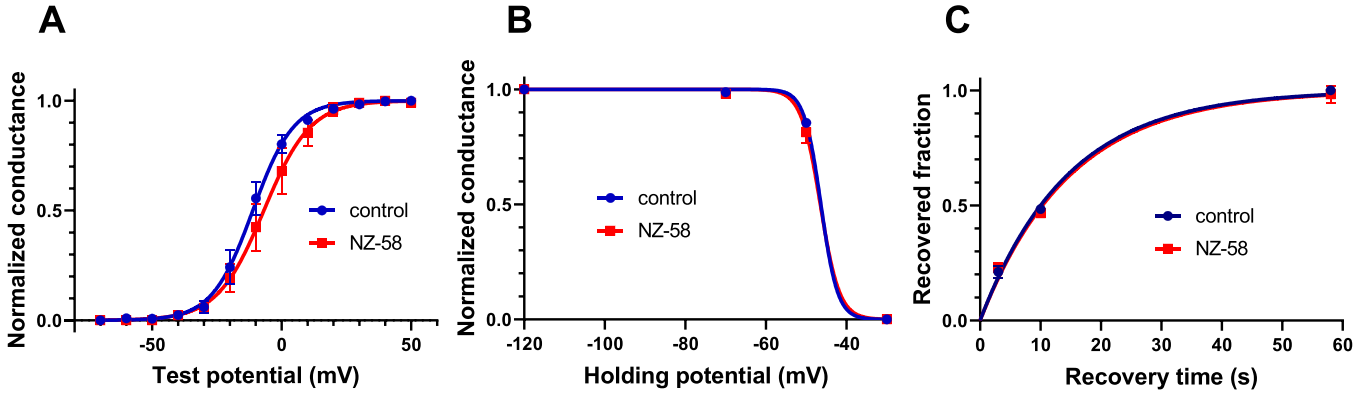

Fig. 10. Voltage-dependence of steady-state activation and inactivation and recovery from inactivation in $K_V1.3$. (A) G-V curves were constructed from I-V relationships using increasing step depolarizations in the absence and presence of 10 μM NZ-58. Blue symbols: control, red symbols: NZ-58 (B) Depolarizations to + 50 mV were used to determine the fraction of available channels at various holding potentials. To avoid rundown effects the protocol was reduced to four holding voltages and 5 μM NZ-58 was applied. (C) Recovery from inactivation was measured by pulse pairs separated by increasing recovery periods at −100 mV. The fraction of recovered channels is plotted as a function of recovery time. Similarly to (B), the number of pulse pairs was reduced to shorten the protocol and 5 μM NZ-58 was used.

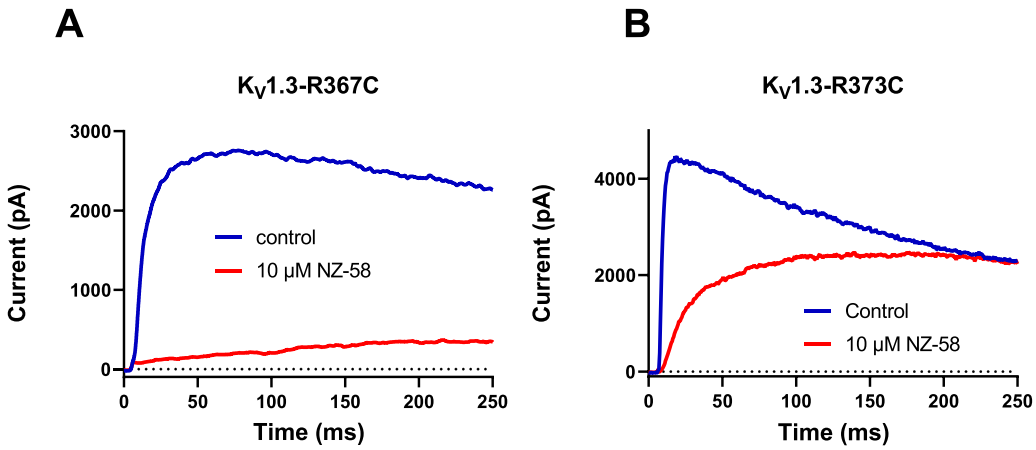

Fig. 11. Effect of NZ-58 on mutant K_V1.3 channels. (A) K_V1.3 currents measured in CHO cells transfected the R367C (R2) mutant. (B) K_V1.3 currents measured in CHO cells transfected the R373C (R4) mutant. Blue: control, red: 10 μM NZ-58 applied from the intracellular side.

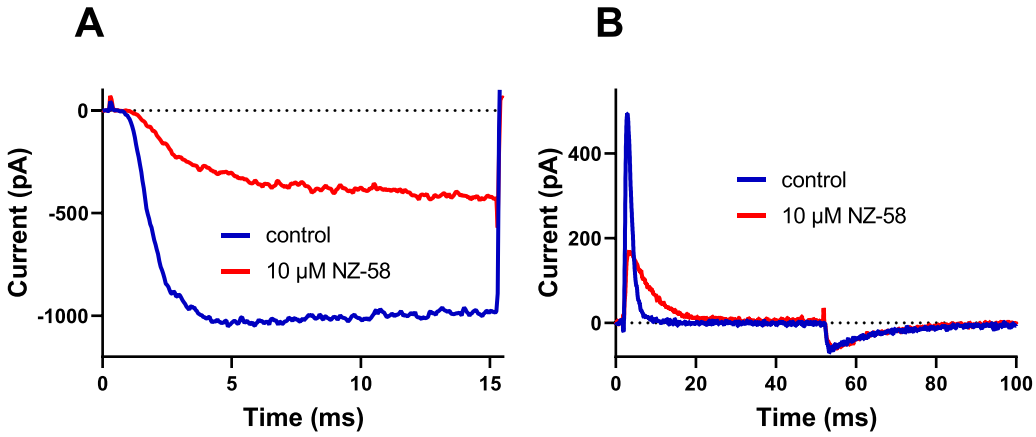

Fig. 12. Inside-out and gating current recordings in K_V1.3. (A) K_V1.3 currents measured in transfected CHO cells in inside-out configuration. Blue: control, red: 10 μM NZ-58 applied from the intracellular side. (B) Gating currents recorded from a CHO cell transfected with K_V1.3-W384F channels, induced by depolarizations to + 40 mV, from a holding potential of −100 mV and then stepped back to −100 mV. Blue: control, red: 10 μM NZ-58.

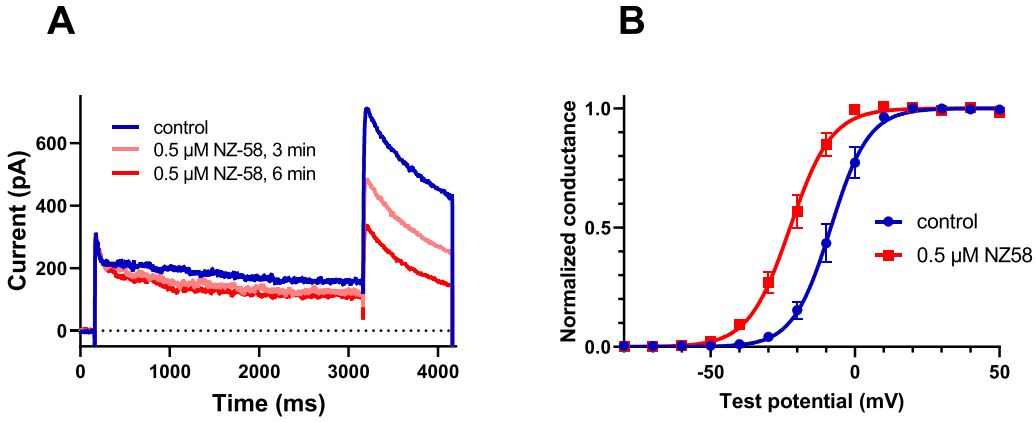

Fig. 13. Effect of NZ-58 on hERG currents. (A) hERG currents were measured on HEK cells stably expressing the channels. The blocking effect of the compound was monitored by the decrease of the tail currents upon stepping back to −40 mV. (B) G-V curves were constructed from peak tail currents at −60 mV, following depolarizing steps to the indicated test potentials.

3.6. Effects on hERG

A noteworthy exception among VGICs was the hERG (K_V11.1) channel with its unique gating, characterized by slow opening, followed by fast inactivation during depolarization. Due to its distinctive gating features, we expected different effects compared to the other VGICs, therefore we explored the gating changes in more detail. Unlike the other K_V and Na_V channels, its activation kinetics were not slowed by NZ-58 and even showed a slight accelerating tendency (τ_{cont} = 208 ± 7 ms, τ_{NZ} = 171 ± 15 ms, n = 5, p = 0.08), although due to the cell-

to-cell variability of current kinetics during depolarizing pulse, this parameter could not be assessed in all cells. During repolarization to −40 mV, the channels inactivated by the depolarization quickly return from inactivation and deactivate generating a tail-current. While the rate of recovery was slightly accelerated ($\tau_{cont} = 9.55 \pm 0.49$ ms, $\tau_{NZ} = 8.71 \pm 0.38$ ms, $n = 6$, $p = 0.01$), the rate of channel closure was not affected by NZ-58 ($\tau_{cont} = 949 \pm 90$ ms, $\tau_{NZ} = 887 \pm 123$ ms, $n = 5$, $p = 0.23$). Surprisingly, the G-V function characterizing the voltage-dependence of activation was significantly left-shifted by the compound ($V_{0.5,cont} = -8.3 \pm 2.1$ mV, $V_{0.5,NZ} = -22.4 \pm 2.0$ mV, $p = 0.009$), in contrast to the other VGICs. In addition, hERG was more sensitive to NZ-58, as 0.5 μM was sufficient to induce the described changes in gating and significantly suppress the current amplitude.

4. Discussion

4.1. Comparison of NZ-58 effects on H_v1 and other VGICs

We originally described NZ-58 as an inhibitor of the H_V1 proton channel [18], which, despite its resemblance to the "traditional" VGICs, has a very distinct structure and function. Notably, H_V1 consists of a single VSD and it lacks a pore through which other VGICs conduct the permeating ions. Accordingly, some of the observed effects induced by NZ-58 were similar in H_V1 and other VGICs, but there were also substantial differences. In H_V1 we described a dual effect on the two components of channel activation: a slowing of the slow component and speeding of the fast component, which resulted in an overall faster activation kinetics. This is in sharp contrast with the drastic slowing of activation kinetics observed in all the tested K_V and Na_V channels. Moreover, deactivation kinetics were significantly accelerated in H_V1, but were unaffected in $Na_V1.5$ and $K_V1.3$. Additionally, NZ-58 induced a right-shift in the voltage-dependence of channel activation of H_V1, which was absent in $Na_V1.5$ and $K_V1.3$. These observations suggest different modes of action in H_V1 and the other VGICs. As H_V1 only consists of segments S1-S4, corresponding to the VSD of classical voltage-gated channels, NZ-58 must bind to the VSD in H_V1 and, based on the effects described above, is likely to bind to it in the other VGICs as well. However, our mutant analysis and docking calculations for H_V1 indicated a binding site involving the selectivity filter and proton permeation pathway, but not any of the gating arginines [18], whereas the lack of other obvious conserved VSD regions in the other VGICs suggested the involvement of these residues in binding. In spite of this, both the R2- and R4-mutant $K_V1.3$ and the DIV-R4 mutant $Na_V1.5$ channels maintained their affinity for NZ-58. We did not observe any major change in $Na_V1.5$, however, in this channel, the mutation affects only one VSD, the one responsible for inactivation, so a weaker effect is expected. In the $K_V1.3$ mutants, where the mutations were present in all four VSDs, the effects became more prominent manifested as even slower activation kinetics and due to the overlap with inactivation, consequently more reduced amplitudes than in the wild type. Therefore, the arginines may indeed be involved in the interaction with NZ-58, even if weakening it rather than enhancing, and other residues are likely to have greater contributions considering the modest change brought on by the mutations.

4.2. Effects on gating kinetics: comparison of $Na_V1.5$ and $K_V1.3$

Studying the effect of NZ-58 in parallel on $Na_V1.5$ and $K_V1.3$ provided an interesting insight into the mechanism, considering the similarities and differences in the structure and function of the two channels. While they have homologous structures, $K_V1.3$ consists of four identical subunits having identical voltage-dependences, kinetics and possibly providing four identical binding sites, $Na_V1.5$, on the other hand, contains four domains with very different voltage-dependences, kinetics and possibly binding sites with different affinities and accessibilities in various gating states [33].

In both channels, NZ-58 induced a robust slowing of channel opening, which requires the activation of DI-DIII VSDs in $Na_V1.5$, and that of all four VSDs in $K_V1.3$. Thus, if NZ-58 binding slows VSD activation, this is expected in both channel types. By contrast, the fast, N-type inactivation of $Na_V1.5$ was similarly slowed, but the slow, C-type inactivation of $K_V1.3$ was oppositely and much less affected. This is not surprising, as fast inactivation in Na_V channels is linked to DIV-VSD activation, while C-type inactivation in K_v channels occurs in the selectivity filter with a much less direct connection to VSD movement. Therefore, if binding of NZ-58 slows VSD activation, slower inactivation is expected in Na_V, but not in K_V channels. The slight acceleration of slow inactivation in $K_V1.3$ may be due to allosteric modulation of the selectivity filter by the compound or simply the result of reduced occupancy of the K^+ ion binding sites controlling inactivation due to the slow opening of the channel and concomitant decreased current. Along the same lines, recovery from inactivation linked to VSD-movements was slowed in $Na_V1.5$, but not affected in $K_V1.3$ where recovery is also allosterically modulated by the VSDs.

The simultaneous slowing of both activation and inactivation in $Na_v1.5$ resulted in a variable concentration- and time-dependent change in the current amplitude, often causing an increase, while the slowing of activation and acceleration of inactivation in $K_V1.3$ always resulted in amplitude reduction. At 50 μM, the extreme slowing of activation was dominant in all channels, which allowed a direct transition to the inactivated state via a brief occupancy of the open state, resulting in almost complete current suppression. Due to its very slow inactivation rate, $K_V1.5$ maintained a sizeable current fraction (Fig. 1C). The slowing of $Na_V1.5$ current inactivation slowed and saturated more quickly than its activation (Fig. 5), which may be explained by the fact that channel opening requires the activation of three VSDs, while inactivation requires the activation of only one VSD. Therefore, the binding sites affecting inactivation may saturate more quickly than the three times as many sites affecting activation. At high concentrations, all sites saturate quickly resulting in dominant slowing of channel opening and the consequent amplitude reduction.

The fact that channel opening of both $Na_V1.5$ and $K_v1.3$ was significantly slowed by NZ-58, but channel closing was not affected, seems surprising, as many effects slowing forward rates speed up backward rates, which should manifest as a faster tail current decay. For example, extracellular acidification causes a right shift in the G-V relationship via the surface charge screening effect and slows current activation and speeds channel closing, as both the VSDs and the pore sense a voltage more negative than what is applied [34]. A similar effect is achieved by several known gating-modifier peptide toxins, for example hanatoxin [35], which shift the G-V curve to the right by binding to the VSD and stabilizing its resting position, thereby slowing opening and speeding closing. It is important to note that during the opening of most K_V channels, each VSD must complete the resting (R) to activated (A) transition, which is followed by a concerted opening step. Although the great majority of gating charge moves during the R to A transitions, a minute VSD motion is also associated with the concerted pore opening (and closing) step, giving it a slight voltage-dependence. Besides stabilizing the R state of the VSDs, hanatoxin also affects this final concerted transition.

Effects, which raise the activation energy for both the forward and backward rates between the R and A states would exert a general slowing of VSD movements, and the observable effects on current activation and deactivation kinetics would depend on the relative rates of these transitions. The effects of NZ-58 can be explained by a direct modulation of VSD movement rather than an interaction with the pore. During opening of K_V channels, activation of the VSDs is faster and precedes the rate-limiting pore opening. However, sufficient slowing of VSD activation by NZ-58 can make this step rate-limiting and thus result in slower channel opening. In contrast, during hyperpolarization, the pore closure, unaffected by NZ-58, precedes the return of the VSDs to the resting state, meaning that the decay of the ionic current is not affected,

regardless of which transition is rate-limiting. Considering the rate-limiting nature of the VSD return in wild type K_V channels during repolarization [36], one would expect a slowing of the OFF gating currents if VSD return is slowed by the compound. However, we have previously shown in the closely related *Shaker* channel that while in the conducting wild type channel pore closing is much faster than charge return, in the permanently inactivated non-conducting W434F mutant (equivalent of K_V1.3 W384F used in this study), the opposite is observed, as pore closing becomes sufficiently slow to become rate-limiting [36]. Since the rate-limiting pore closure is unaffected by NZ-58, the subsequent charge return and consequently OFF gating kinetics are not affected either. Alternatively, the backward transition of the VSDs is in fact not affected by NZ-58, which, in light of the strong effect on the forward rates, seems unlikely. The slowing of the VSD-linked recovery from inactivation in Na_V1.5 also argues against this scenario [37]. Although gating current measurements were carried out in K_V1.3, the fact that the maximal gating charge was not affected by NZ-58, as opposed to a 38% reduction induced by lidocaine in Na_V1.5 [38], argues against a trapping mechanism and supports a simple slowing action of the VSDs.

Given that both the G-V and the SSI curves were unaffected by NZ-58 in both Na_V1.5 and K_V1.3 channels further supports the idea that NZ-58 binding causes only the slower movement of the VSDs locally, rather than causing larger scale conformational changes that would affect the energetics of the gating states.

As NZ-58 was equally effective in whole-cell and inside-out patch configurations, and considering its lipophilic nature and its ability to easily cross the membrane, the sidedness of the binding site accessibility is difficult to predict. Since application of NZ-58 to the closed channels induced the same kinetic changes as when channels were exposed to it in the closed, open and inactivated states due to continuous pulsing, it is reasonable to assume that it can bind to the VSD even in its resting state, when it is mostly buried in the membrane.

4.3. Unique effects on the hERG channel

The hERG (K_V11.1) channel is a critical player in the repolarization phase of the cardiac action potential and belonging to the K_V family it shares the main structural elements with the Shaker-type (K_V1.x) channels. However, it has some distinctive structural and functional features that may explain its unique responses to NZ-58 [39–41]. As its central cavity is unusually large and rich in aromatic residues, hERG is notorious for causing off-target side effects by a wide range of drugs. It is therefore not surprising that NZ-58 caused significant inhibition even at 0.5 μM. However, unlike the other VGICs, its gating kinetics were not significantly affected, but its G-V function was left-shifted. Detailed characterization would take many more experiments, but its distinctive gating features can explain some observations. Compared to K_V1.3, hERG has a much looser connection between the VSD and the pore, so during opening, VSD movement is much faster than the rate-limiting pore opening, which is followed by a quick transition to the inactivated state. This explains the lack of effect on channel opening kinetics. In addition, an N-terminal PAS domain and a C-terminal Cyclic Nucleotide–Binding Homology domain regulate deactivation kinetics, which results in a similarly weak link between VSD return and the very slow channel closing. Therefore, an effect on the VSD is not necessarily expected to manifest on the deactivation kinetics. The presence of multiple binding sites is also plausible, and the current reduction at low NZ-58 concentration may originate from inhibition in the cavity.

4.4. Unique binding site(s) and mechanism

Na_V channels are the initiators of action potentials in neurons, skeletal and cardiac muscle cells, and as such, their mutations are involved in pathologies related to excitable tissues such as epilepsies and intellectual disabilities (Na_V1.1–1.3 and 1.6), myotonia and paralysis (Na_V1.4), cardiac arrhythmias (Na_V1.5) and pain disorders (Na_V1.7–1.9). Accordingly, drugs developed for the treatment of these diseases target the underlying Na_V channels [13].

Several typical binding sites of modulator compounds have been identified in Na_V channels (reviewed recently in [17,42]), which could be more precisely defined with the advent of high-resolution cryo--electron microscopy structures. A systematic structural atlas was recently created to aid in accurately identifying these binding sites [43]. Most clinically used drugs targeting Na_V channels, such as anti-arrhythmic agents and local anesthetics, bind in the central cavity [17,44,45], while the best-known small molecule Na_V inhibitor, tetrodotoxin, and some peptide blockers, such as μ-conotoxin KIIIA, obstruct the permeation pathway at the selectivity filter in the extracellular entrance of the pore [46,47]. Further sites are located along the permeation pathway at and below the activation gate, as well as sites accessible via the lipid phase through fenestrations [43].

As opposed to the central cavities of Na_V isoforms, which show high homology, the VSDs are much more distinct and therefore are more suitable for specific targeting [17]. Yet, currently much fewer modulators are known to target the VSDs, and most of those are gating modifier toxins from animal venoms. Traditionally named “receptor site 3” located extracellularly on the DIV-VSD, is a binding site for α-scorpion toxins, which inhibit the fast inactivation of the channels by trapping the VSD in an intermediate conformation [48]. “Receptor site 4” is found on the DII-VSD and mostly targeted by β scorpion and spider toxins [17], which may have either excitatory or inhibitory effects depending on whether they stabilize the VSD in the activated or the resting state. In contrast, the DI and DIII VSDs are much less targeted by natural toxins, possibly due to the reduced accessibility caused by the presence of auxiliary β-subunits [43]. Recently, highly specific aryl sulfonamide compounds have been developed with the aim to treat chronic pain via Na_V1.7 inhibition, which bind to and stabilize the DIV-VSD in the activated conformation, keeping the channel inactivated [49]. However, despite the promising high selectivity, clinical trials have not yet proven their applicability. In contrast, suzetrigine (VX-548) became the first FDA-approved selective Na_V1.8 inhibitor for acute pain management [50]. It binds to the DII-VSD of Na_V1.8 preferably in its resting conformation, stabilizing it and thereby preventing channel opening. Interestingly, unlike many other Na_V inhibitors, it displays reverse use-dependence, meaning that its effectiveness declines with repetitive or strong depolarizations.

Most known Na_V modulators inhibit channel function and in clinical settings, their goal is to suppress hyperexcitability associated with gain-of-function mutations, as e.g. in Na_V1.5 causing LQT3 syndrome. However, often enhancement of channel function is desired, as in the case of loss-of-function mutations, causing Brugada syndrome. Besides the peptide toxin activators mentioned above, some small molecule Na_V activators are also known, including batrachotoxin, aconitine and grayanotoxin, which bind in the central cavity preferably in the open state of the channel, and among other effects, they shift the voltage-dependence of activation in the negative direction [51]. Veratridine has a similar effect and binding site, except that it does not require repetitive depolarizations for binding. Small molecule Na_V activators, such as pyrethrins, are also used as insecticides, inducing spastic paralysis via enhanced Na^+ influx.

Thus, despite the abundance of known Na_V-modulating compounds, only a minority of them bind to the VSDs, which may offer more specific targets for modulation than the cavity. However, the mechanisms of action of these modulators listed above significantly differ from that of NZ-58, especially considering its enhancing effect at low concentrations. Comparison with small molecule activators also reveals completely different binding sites, effects on gating, and state-dependence of binding. We are not aware of any other modulators that affect only the speed of VSD movements, but not the energetics of the states. Thus, both the binding site and the mechanism of action seem to be unique for NZ-58. Although it potently blocked the hERG channel, it is also worth

noting that the induced effects were completely different compared to other VGICs, which may suggest a pattern for the design of molecules targeting specific VGICs while avoiding the often-encountered side effect on hERG.

4.5. NZ-58 as a prospective lead molecule?

Although NZ-58 has an inhibitory effect on most of the tested channels in this study via slowing channel opening, at low concentrations it significantly enhances the activity of Na_V channels, the increase in Na^+ influx amounting to about 22% even at 0.5 μM. This enhancement was also observed in the loss-of-function Brugada mutant. Such activity has significant therapeutic potential in the case of Na_V loss-of-function related pathologies, as demonstrated by the rescue of Dravet-syndrome mice by a spider venom peptide activator of the loss-of-function mutant $Na_V1.1$ channels [52].

As shown by the above results, NZ-58 is far from being isoform selective. It is not even selective for channel type, as revealed by testing it on a number of different channels. Unfortunately, many publications reporting the discovery of new ion channel modulating compounds often completely neglect selectivity checks or limit them to isoforms of the same channel family, failing to expand testing to other channel types. Over time, this may lead to the mischaracterization of such compounds as "selective inhibitors", which are then used in functional tests leading to false conclusions on the role of specific ion channels [26, 53].

Although isoform selectivity is a highly desirable trait of potential lead molecules in order to avoid side effects due to off-target actions, the reality is that the majority of clinically used VGIC modulator compounds are "dirty drugs" affecting multiple targets [54]. Nevertheless, despite their narrow therapeutic windows, their administration still achieves therapeutic goals, justifying their use. For example, lidocaine blocks multiple Na_V isoforms and is used as a local anesthetic despite its inhibitory effect on the cardiac $Na_V1.5$ channel [38,55]. Verapamil, which targets voltage-gated Ca^{2+} channels to treat hypertension and angina pectoris, also blocks Na_V [56,57] and K_V channels [58]. The Class III antiarrhythmic drug amiodarone blocks K_V, ligand-gated K^+, Na_V and Ca_V channels and as a result affects almost every phase of the cardiac action potential [12,59]. These examples illustrate that careful dosing and the appropriate delivery route can beneficially exploit even a narrow therapeutic window. In addition, the multi-target nature of a drug molecule may even become advantageous, e.g. in suppressing cancer cell progression, which can rely on the overexpression of multiple VGICs, including e.g. H_V1 for pH control and specific others for setting the appropriate membrane potential or ion concentrations [7,60,61]. In these cases, a synergistic inhibitory effect may yield beneficial results.

5. Conclusion

In this work, we characterized a small molecule, NZ-58, as a pan-VSD modulator, acting on all tested voltage-gated ion channels, while showing no effect on non-voltage gated ones. We highlighted both the similarities and differences in its actions on Na_V and K_V channels and demonstrated that at low micromolar concentrations, it acts as a potent activator of Na_V channels, including a Brugada-mutant $Na_V1.5$. This represents a desirable property for the potential treatment of pathologies caused by loss-of-function mutations. Although its lack of selectivity makes NZ-58 an unlikely lead compound, its exceptional gating effects and novel binding site may provide new opportunities for the search for isoform- and function-specific modulators of voltage-gated ion channels.

Institutional review board statement

Experiments on human B cells were carried out under the approval of the University of Debrecen Regional Research Ethical Committee (DE RKEB/IKEB 5228–2019), and informed consent has been obtained as a part of the ethical approval.

CRediT authorship contribution statement

Nace Zidar: Writing – review & editing, Resources, Funding acquisition, Conceptualization. **Russo Teklu Teshome:** Investigation, Data curation. **Adam Feher:** Writing – review & editing, Investigation, Data curation. **Tihomir Tomašič:** Writing – review & editing, Formal analysis, Conceptualization. **Geraldo Jorge Domingos:** Writing – review & editing, Writing – original draft, Investigation, Funding acquisition, Data curation, Conceptualization. **Martina Piga:** Writing – review & editing, Resources, Conceptualization. **Norbert Szentandrássy:** Writing – review & editing, Funding acquisition. **Zoltan Varga:** Writing – review & editing, Writing – original draft, Resources, Project administration, Methodology, Investigation, Funding acquisition, Formal analysis, Data curation, Conceptualization. **Shahrukh Husain:** Investigation, Data curation. **Al Olaimi Amna:** Writing – review & editing, Investigation. **Ferenc Papp:** Writing – review & editing. **Zsigmond Máté Kovács:** Writing – review & editing, Investigation. **Rama Elian:** Investigation. **Zsigmond Vizi:** Investigation, Funding acquisition, Data curation. **Bangera Kavya C:** Investigation, Data curation.

Declaration of Competing Interest

The authors declare that they have no known competing financial interests or personal relationships that could have appeared to influence the work reported in this paper.

Acknowledgements

This research work was conducted with the support of the Stipendium Hungaricum Scholarship by the Tempus Public Foundation (G.J.D) and the National Academy of Scientist Education Program of the National Biomedical Foundation under the sponsorship of the Hungarian Ministry of Culture and Innovation (ZS.V).

Project no. 2024–1.2.3-HU-RIZONT-2024–00099 has been implemented with the support provided by the Ministry of Culture and Innovation of Hungary from the National Research, Development, and Innovation Fund, financed under the 2024–1.2.3-HU-RIZONT funding scheme.

This study was funded by the following grants: National Research Development and Innovation Office, Hungary, grants OTKA K132906 (Z.V.), 2025–1.2.4-T É T-2025–00007 (Z.V.) and NKFIH K142764 (N. S.).

This work was supported by the Slovenian Research Agency (Grant No. P1–0208) and the University of Debrecen program for scientific publication.

The work of our technician, Cecilia Nagy, is highly appreciated.

Appendix A. Supporting information

Supplementary data associated with this article can be found in the online version at doi:10.1016/j.biopha.2026.119530.

Data availability

Data will be made available on request.

References

[1] J. Huang, X. Pan, N. Yan, Structural biology and molecular pharmacology of voltage-gated ion channels, Nat. Rev. Mol. Cell Biol. 25 (11) (2024) 904–925.
[2] B. Hille. Ion channels of excitable membranes, Third edition ed., Sinauer Associates is an imprint of Oxford University Press, Sunderland, MA, USA, 2001.
[3] M. Sasaki, M. Takagi, Y. Okamura, A voltage sensor-domain protein is a voltage-gated proton channel, Science 312 (5773) (2006) 589–592.

[4] I.S. Ramsey, M.M. Moran, J.A. Chong, D.E. Clapham, A voltage-gated proton-selective channel lacking the pore domain, Nature 440 (7088) (2006) 1213–1216.
[5] Y. Liu, C. Li, J.A. Freites, D.J. Tobias, G.A. Voth, Quantitative insights into the mechanism of proton conduction and selectivity for the human voltage-gated proton channel Hv1, Proc. Natl. Acad. Sci. 121 (38) (2024) e2407479121.
[6] F. Tombola, M.H. Ulbrich, E.Y. Isacoff, Architecture and gating of Hv1 proton channels, J. Physiol. 587 (Pt 22) (2009) 5325–5329.
[7] J.J. Alvear-Arias, A. Pena-Pichicoi, C. Carrillo, M. Fernandez, T. Gonzalez, J. A. Garate, C. Gonzalez, Role of voltage-gated proton channel (Hv1) in cancer biology, Front. Pharmacol. 14 (2023) 1175702.
[8] P.V. Lishko, Y. Kirichok, The role of Hv1 and CatSper channels in sperm activation, J. Physiol. 588 (Pt 23) (2010) 4667–4672.
[9] I.S. Ramsey, E. Ruchti, J.S. Kaczmarek, D.E. Clapham, Hv1 proton channels are required for high-level NADPH oxidase-dependent superoxide production during the phagocyte respiratory burst, Proc. Natl. Acad. Sci. 106 (18) (2009) 7642–7647.
[10] C. Arreola-Mora, J. Silva-Pereyra, T. Fernandez, M. Paredes-Cruz, B. Bertado-Cortes, I. Grijalva, Effects of 4-aminopyridine on attention and executive functions of patients with multiple sclerosis: randomized, double-blind, placebo-controlled clinical trial, Prelim. Rep. Mult. Scler. Relat. Disord. 28 (2019) 117–124.
[11] D. Lopez-Mateos, B.J. Harris, A. Hernandez-Gonzalez, V. Yarov-Yarovoy, H. Wulff, Recent advances in the pharmacology of voltage-gated ion channels, Pharmacol. Rev. 77 (6) (2025) 100090.
[12] I. Gelman, N. Sharma, O. McKeeman, P. Lee, N. Campagna, N. Tomei, A. Baranchuk, S. Zhang, M. El-Diasty, The ion channel basis of pharmacological effects of amiodarone on myocardial electrophysiological properties, a comprehensive review, Biomed. Pharmacother. 174 (2024) 116513.
[13] W.A. Catterall, M.J. Lenaeus, T.M. Gamal El-Din, Structure and pharmacology of voltage-gated sodium and calcium channels, Annu. Rev. Pharmacol. Toxicol. 60 (2020) 133–154.
[14] C. Fairhurst, F. Martin, I. Watt, M. Bland, T. Doran, W.J. Brackenbury, Sodium channel-inhibiting drugs and cancer-specific survival: a population-based study of electronic primary care data, BMJ Open 13 (2) (2023) e064376.
[15] N. Aoki-Shioi, S. Nomura, Y. Tanaka, S. Hirose, Ion channel-targeting toxins: structural mechanisms of activation, inhibition, and therapeutic potential, Toxins 17 (12) (2025).
[16] V.F. Palmisano, N. Anguita-Ortiz, S. Faraji, J.J. Nogueira, Voltage-gated ion channels: structure, pharmacology and photopharmacology, Chemphyschem a Eur. J. Chem. Phys. Phys. Chem. 25 (16) (2024) e202400162.
[17] G. Wisedchaisri, T.M.Gamal El-Din, Druggability of voltage-gated sodium channels-exploring old and new drug receptor sites, Front. Pharmacol. 13 (2022) 858348.
[18] M. Piga, Z. Varga, A. Feher, F. Papp, E. Korpos, K.C. Bangera, R. Frlan, J. Ilas, J. Dernovsek, T. Tomasic, N. Zidar, Identification of a novel structural class of H(V) 1 inhibitors by structure-based virtual screening, J. Chem. Inf. Model. (2024).
[19] T.E. Decoursey, K.G. Chandy, S. Gupta, M.D. Cahalan, Voltage-gated K + channels in human T lymphocytes: a role in mitogenesis? Nature 307 (1984) 465–468.
[20] D.R. Matteson, C. Deutsch, K channels in T lymphocytes: a patch clamp study using monoclonal antibody adhesion, Nature 307 (1984) 468–471.
[21] G. Panyi, Z.F. Sheng, L.W. Tu, C. Deutsch, C-type inactivation of a voltage-gated K + channel occurs by a cooperative mechanism, Biophys. J. 69 (3) (1995) 896–904.
[22] J. López-Barneo, T. Hoshi, S.H. Heinemann, R.W. Aldrich, Effects of external cations and mutations in the pore region on C-type inactivation of Shaker potassium channels, Recept. Channels 1 (1993) 61–71.
[23] A. Tyagi, T. Ahmed, S. Jian, S. Bajaj, S.T. Ong, S.S.M. Goay, Y. Zhao, I. Vorobyov, C. Tian, K.G. Chandy, S. Bhushan, Rearrangement of a unique Kv1.3 selectivity filter conformation upon binding of a drug, Proc. Natl. Acad. Sci. 119 (5) (2022).
[24] A.L. Hodgkin, A.F. Huxley, A quantitative desription of membrane current and its application to conduction and excitation in nerve, J. Physiol. 117 (1952) 500–544.
[25] M. Chahine, A.L. George Jr., M. Zhou, S. Ji, W. Sun, R.L. Barchi, R. Horn, Sodium channel mutations in paramyotonia congenita uncouple inactivation from activation, Neuron 12 (2) (1994) 281–294.
[26] T.G. Szanto, A. Feher, E. Korpos, A. Gyöngyösi, J. Kállai, B. Mészáros, K. Ovari, Á. Lányi, G. Panyi, Z. Varga, 5-Chloro-2-Guanidinobenzimidazole (ClGBI) Is a Non-Selective Inhibitor of the Human HV1 Channel, Pharmaceuticals 16 (2023).
[27] Z. Varga, G. Gurrola-Briones, F. Papp, R.C. Rodriguez de la Vega, G. Pedraza-Alva, R.B. Tajhya, R. Gaspar, L. Cardenas, Y. Rosenstein, C. Beeton, L.D. Possani, G. Panyi, Vm24, a natural immunosuppressive peptide, potently and selectively blocks Kv1.3 potassium channels of human T cells, Mol. Pharm. 82 (3) (2012) 372–382.
[28] H. Liu, J.H. Naismith, An efficient one-step site-directed deletion, insertion, single and multiple-site plasmid mutagenesis protocol, BMC Biotechnol. 8 (2008) 91.
[29] F. Zakany, P. Pap, F. Papp, T. Kovacs, P. Nagy, M. Peter, L. Szente, G. Panyi, Z. Varga, Determining the target of membrane sterols on voltage-gated potassium channels, Biochim. Et. Biophys. Acta Mol. Cell Biol. Lipids 1864 (3) (2019) 312–325.
[30] T. Nakajima, Y. Kaneko, A. Saito, M. Ota, T. Iijima, M. Kurabayashi, Enhanced fast-inactivated state stability of cardiac sodium channels by a novel voltage sensor SCN5A mutation, R1632C, as a cause of atypical Brugada syndrome, Heart Rhythm 12 (11) (2015) 2296–2304.
[31] M. Piga, G.J. Domingos, A. Feher, F. Papp, K.C. Bangera, Z. Varga, F. Zakany, T. Kovacs, J. Dernovsek, T. Tomasic, N. Zidar, Targeting voltage-gated proton channel H(V)1: optimised 5-phenyl-2-aminoimidazoles with anticancer potential, Eur. J. Med. Chem. 297 (2025) 117936.
[32] S. Jo, B.P. Bean, Sidedness of carbamazepine accessibility to voltage-gated sodium channels, Mol. Pharm. 85 (2) (2014) 381–387.
[33] Z. Varga, W. Zhu, A.R. Schubert, J.L. Pardieck, A. Krumholz, E.J. Hsu, M. A. Zaydman, J. Cui, J.R. Silva, Direct measurement of cardiac Na+ channel conformations reveals molecular pathologies of inherited mutations, Circ. Arrhythmia Electrophysiol. (2015).
[34] S. Somodi, Z. Varga, P. Hajdu, J.G. Starkus, D.I. Levy, R. Gaspar, G. Panyi, pH dependent modulation of Kv1.3 inactivation: the role of His399, Am. J. Physiol. Cell Physiol. 287 (2004) C1067–C1076.
[35] K.J. Swartz, Tarantula toxins interacting with voltage sensors in potassium channels, Toxicon 49 (2) (2007) 213–230.
[36] Z. Varga, M.D. Rayner, J.G. Starkus, Cations affect the rate of gating charge recovery in wild-type and W434F Shaker channels through a variety of mechanisms, J. Gen. Physiol. JID - 2985110R 119 (5) (2002) 467–485.
[37] E.J. Hsu, W. Zhu, A.R. Schubert, T. Voelker, Z. Varga, J.R. Silva, Regulation of Na(+) channel inactivation by the DIII and DIV voltage-sensing domains, J. Gen. Physiol. 149 (3) (2017) 389–403.
[38] M.F. Sheets, D.A. Hanck, Molecular action of lidocaine on the voltage sensors of sodium channels, J. Gen. Physiol. 121 (2) (2003) 163–175.
[39] W. Wang, R. MacKinnon, Cryo-EM structure of the open human Ether-a-go-go-Related K(+) Channel hERG, Cell 169 (3) (2017) 422–430, e10.
[40] M.C. Sanguinetti, C. Jiang, M.E. Curran, M.T. Keating, A mechanistic link between an inherited and an acquired cardiac arrhythmia: HERG encodes the IKr potassium channel, Cell 81 (2) (1995) 299–307.
[41] J.W. Warmke, B. Ganetzky, A family of potassium channel genes related to eag in Drosophila and mammals, Proc. Natl. Acad. Sci. USA 91 (8) (1994) 3438–3442.
[42] M. Alsaloum, S.D. Dib-Hajj, D.A. Page, P.C. Ruben, A.R. Krainer, S.G. Waxman, Voltage-gated sodium channels in excitable cells as drug targets, Nat. Rev. Drug Discov. 24 (5) (2025) 358–378.
[43] Z. Li, Q. Wu, N. Yan, A structural atlas of druggable sites on Na(v) channels, Channels (Austin) 18 (1) (2024) 2287832.
[44] D. Jiang, H. Shi, L. Tonggu, T.M. Gamal El-Din, M.J. Lenaeus, Y. Zhao, C. Yoshioka, N. Zheng, W.A. Catterall, Structure of the cardiac sodium channel, Cell 180 (1) (2020) 122–134, e10.
[45] T.M. Gamal El-Din, M.J. Lenaeus, N. Zheng, W.A. Catterall, Fenestrations control resting-state block of a voltage-gated sodium channel, Proc. Natl. Acad. Sci. 115 (51) (2018) 13111–13116.
[46] H. Shen, Z. Li, Y. Jiang, X. Pan, J. Wu, B. Cristofori-Armstrong, J.J. Smith, Y.K. Y. Chin, J. Lei, Q. Zhou, G.F. King, N. Yan, Structural basis for the modulation of voltage-gated sodium channels by animal toxins, Science 362 (6412) (2018).
[47] X. Pan, Z. Li, X. Huang, G. Huang, S. Gao, H. Shen, L. Liu, J. Lei, N. Yan, Molecular basis for pore blockade of human Na(+) channel Na(v)1.2 by the mu-conotoxin KIIIA, Science 363 (6433) (2019) 1309–1313.
[48] T. Clairfeuille, A. Cloake, D.T. Infield, J.P. Llongueras, C.P. Arthur, Z.R. Li, Y. Jian, M.F. Martin-Eauclaire, P.E. Bougis, C. Ciferri, C.A. Ahern, F. Bosmans, D. H. Hackos, A. Rohou, J. Payandeh, Structural basis of alpha-scorpion toxin action on Na(v) channels, Science 363 (6433) (2019).
[49] K. McCormack, S. Santos, M.L. Chapman, D.S. Krafte, B.E. Marron, C.W. West, M. J. Krambis, B.M. Antonio, S.G. Zellmer, D. Printzenhoff, K.M. Padilla, Z. Lin, P. K. Wagoner, N.A. Swain, P.A. Stupple, M. de Groot, R.P. Butt, N.A. Castle, Voltage sensor interaction site for selective small molecule inhibitors of voltage-gated sodium channels, Proc. Natl. Acad. Sci. 110 (29) (2013) E2724, 32.
[50] M. Jones, A. Demery, R.A. Al-Horani, Suzetrigine: a novel non-opioid analgesic for acute pain management-a review, Drugs Drug Candidates 4 (3) (2025).
[51] J.R. Deuis, A. Mueller, M.R. Israel, I. Vetter, The pharmacology of voltage-gated sodium channel activators, Neuropharmacology 127 (2017) 87–108.
[52] K.L. Richards, C.J. Milligan, R.J. Richardson, N. Jancovski, M. Grunnet, L. H. Jacobson, E.A.B. Undheim, M. Mobli, C.Y. Chow, V. Herzig, A. Csoti, G. Panyi, C.A. Reid, G.F. King, S. Petrou, Selective NaV1.1 activation rescues Dravet syndrome mice from seizures and premature death, Proc. Natl. Acad. Sci. 115 (34) (2018) E8077–E8085.
[53] A. Bartok, A. Toth, S. Somodi, T.G. Szanto, P. Hajdu, G. Panyi, Z. Varga, Margatoxin is a non-selective inhibitor of human Kv1.3 K+ channels, Toxicon 87 (2014) 6–16.
[54] B. Hegyi, I. Komaromi, P.P. Nanasi, N. Szentandrassy, Selectivity problems with drugs acting on cardiac Na(+) and Ca(2)(+) channels, Curr. Med. Chem. 20 (20) (2013) 2552–2571.
[55] P. Chevrier, K. Vijayaragavan, M. Chahine, Differential modulation of Nav1.7 and Nav1.8 peripheral nerve sodium channels by the local anesthetic lidocaine, Br. J. Pharm. 142 (3) (2004) 576–584.
[56] K. Shigenobu, J.A. Schneider, N. Sperelakis, Verapamil blockade of slow Na+ and Ca++ responses in myocardial cells, J. Pharmacol. Exp. Ther. 190 (2) (1974) 280–288.
[57] L.M. Hondeghem, B.G. Katzung, Time- and voltage-dependent interactions of antiarrhythmic drugs with cardiac sodium channels, Biochim. Biophys. Acta 472 (3-4) (1977) 373–398.
[58] T.E. DeCoursey, Mechanism of K+ channel block by verapamil and related compounds in rat alveolar epithelial cells, J. Gen. Physiol. 106 (4) (1995) 745–779.
[59] I. Kodama, K. Kamiya, J. Toyama, Amiodarone: ionic and cellular mechanisms of action of the most promising class III agent, Am. J. Cardiol. 84 (9A) (1999) 20R–28R.
[60] V.R. Rao, M. Perez-Neut, S. Kaja, S. Gentile, Voltage-gated ion channels in cancer cell proliferation, Cancers 7 (2) (2015) 849–875.
[61] T.K. Leslie, W.J. Brackenbury, Sodium channels and the ionic microenvironment of breast tumours, J. Physiol. 601 (9) (2023) 1543–1553.